environmental microbiology

Environmental Microbiology (2017) **19**(8), 3132–3151 doi:10.1111/1462-2920.13788

Functional structure of the bromeliad tank microbiome is strongly shaped by local geochemical conditions

Stilianos Louca,[1,2*] Saulo M. S. Jacques,[3,4] Aliny P. F. Pires,[3] Juliana S. Leal,[3,5] Angélica L. González,[6] Michael Doebeli[1,2,7] and Vinicius F. Farjalla[3]

[1]*Biodiversity Research Centre, University of British Columbia, Vancouver, BC, Canada.*

[2]*Department of Zoology, University of British Columbia, Vancouver, BC, Canada.*

[3]*Department of Ecology, Biology Institute, Universidade Federal do Rio de Janeiro, Rio de Janeiro, Brazil.*

[4]*Programa de Pós-Graduação em Ecologia e Evolução, Universidade Estadual do Rio de Janeiro, Rio de Janeiro, Brazil.*

[5]*Programa de Pós-Graduação em Ecologia, Universidade Federal do Rio de Janeiro, Rio de Janeiro, Brazil.*

[6]*Biology Department & Center for Computational & Integrative Biology, Rutgers University, Camden, NJ, USA.*

[7]*Department of Mathematics, University of British Columbia, Vancouver, BC, Canada.*

Summary

Phytotelmata in tank-forming Bromeliaceae plants are regarded as potential miniature models for aquatic ecology, but detailed investigations of their microbial communities are rare. Hence, the biogeochemistry in bromeliad tanks remains poorly understood. Here we investigate the structure of bacterial and archaeal communities inhabiting the detritus within the tanks of two bromeliad species, *Aechmea nudicaulis* and *Neoregelia cruenta*, from a Brazilian sand dune forest. We used metagenomic sequencing for functional community profiling and 16S sequencing for taxonomic profiling. We estimated the correlation between functional groups and various environmental variables, and compared communities between bromeliad species. In all bromeliads, microbial communities spanned a metabolic network adapted to oxygen-limited conditions, including all denitrification steps, ammonification, sulfate respiration, methanogenesis, reductive acetogenesis and anoxygenic phototrophy. Overall, CO_2 reducers dominated in abundance over sulfate reducers, and anoxygenic phototrophs largely outnumbered oxygenic photoautotrophs. Functional community structure correlated strongly with environmental variables, between and within a single bromeliad species. Methanogens and reductive acetogens correlated with detrital volume and canopy coverage, and exhibited higher relative abundances in *N. cruenta*. A comparison of bromeliads to freshwater lake sediments and soil from around the world, revealed stark differences in terms of taxonomic as well as functional microbial community structure.

Received 19 October, 2016; accepted 24 April, 2017. *For Correspondence. E-mail louca@zoology.ubc.ca

Introduction

Bromeliads (fam. Bromeliaceae) are plants found throughout the neotropics, with many species having rosette-like foliages that can accumulate water and detritus (e.g. dead leaves from the surrounding canopy) in a central cavity (Kitching, 2001). The accumulation and decomposition of detritus inside these cavities ('tanks') provides nutrients to the plant (Benzing and Renfrow, 1974; Endres and Mercier, 2003; Romero *et al.*, 2006) and to a plethora of organisms residing in the tanks (Srivastava, 2006). In coastal sand dune forests or 'restingas' (Fig. 1A), which cover ~70% of the Brazilian coast, bromeliads can reach densities over 15 000 ha^{-1} and constitute moist and nutrient-rich oases amid a predominantly sandy and nutrient-poor environment (Cogliatti-Carvalho *et al.*, 2001). In such environments, bromeliad tanks are biodiversity hotspots and central hubs for biomass and regional nutrient cycling (Rocha *et al.*, 2000; Romero *et al.*, 2006; Martinson *et al.*, 2010). A great number of organisms, including bacteria, archaea, fungi, protozoans, insects, amphibians and reptiles, spend part or all of their life cycle in these tanks (Rocha *et al.*, 2000). These organisms can engage in a plethora of interactions and ecosystem processes including active nitrogen fixation (Brighigna *et al.*, 1992; Goffredi *et al.*, 2011b; Giongo *et al.*, 2013), photosynthesis (Bouard *et al.*, 2012), chemolithotrophy (Goffredi *et al.*, 2011a), herbivory, predation and detritivory (Ngai and Srivastava,

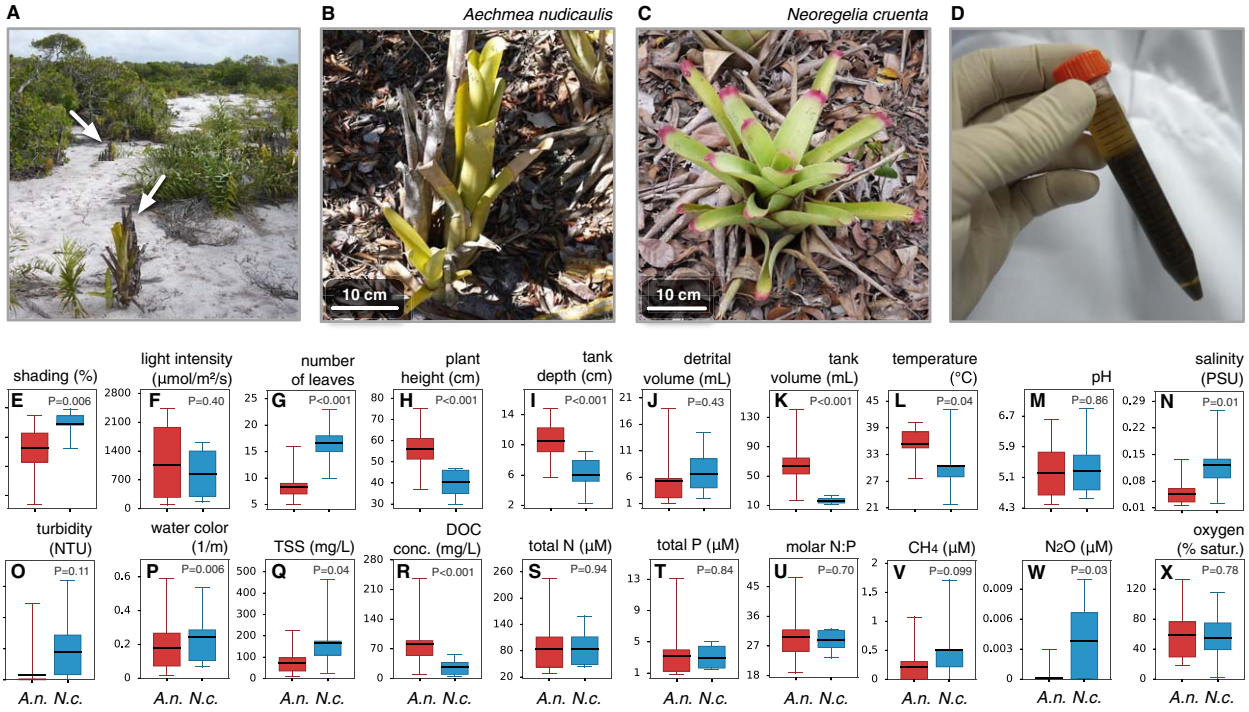

Fig. 1. Sampling site and bromeliads.
A. Sampling site in the Jurubatiba National Park, on the east coast of Brazil.
B. *Aechmea nudicaulis* (also indicated by white arrows in A) and (C) *Neoregelia cruenta*, the two bromeliad species considered in this study and the dominant bromeliad species in Jurubatiba. The rosette-like foliage arrangement forms multiple small peripheral cavities and a larger central tank, which accumulate rainwater, litter and dead animals and support intense nutrient cycling by specialized microbial communities.
D. Detritus extracted from the bottom of a bromeliad tank.
E–X. Box-whisker plots of physical (E–L) and chemical (M–X) variables across 22 *A. nudicaulis* (*A.n.*, red) and 9 *N. cruenta* (*N.c.*, blue) bromeliads. Whiskers show 95% percentiles around the medians. Statistical significances of differences in mean values between *A. nudicaulis* and *N. cruenta* (*P*-values based on permutation tests) are indicated in the plots. [Colour figure can be viewed at wileyonlinelibrary.com]

2006). Extensive research on protist and animal communities in bromeliad tanks reveals a food web structure that is comparable in complexity to much larger aquatic ecosystems (Richardson, 1999; Kitching, 2000; Rocha *et al.*, 2000; Marino *et al.*, 2013). Because bromeliad tanks constitute semi-isolated and self-contained systems, they are considered ideal models for ecosystem ecology, biogeography and climate change research (Srivastava *et al.*, 2004; Farjalla *et al.*, 2012; Atwood *et al.*, 2013; Brandt *et al.*, 2015).

The bulk of organic matter decomposition and nutrient cycling within bromeliad tanks is catalysed by microorganisms (Bouard *et al.*, 2012). Using bromeliad tanks as models for ecosystem ecology thus requires a solid understanding of the microbial component and the biochemical processes that it catalyses. The vast majority of past studies on bromeliad tank communities either exclusively focused on animals or only considered microbial community structure at coarse resolutions, for example, combining all bacteria into a single group (Ngai and Srivastava, 2006; Farjalla *et al.*, 2012; Marino *et al.*, 2013; González *et al.*, 2014). Previous work utilizing denaturation gradient gel electrophoresis (DGGE) revealed rich and highly variable microbial communities without, however, providing detailed information on taxonomic or functional structure (Farjalla *et al.*, 2012). Sequencing of 16S ribosomal RNA (rRNA) clone libraries (Goffredi *et al.*, 2011b) and shotgun environmental mRNA sequencing (Goffredi *et al.*, 2015) have provided further insight on microbial taxonomic composition and on active metabolic pathways in rainforest bromeliads. These studies revealed that decomposition of organic matter leads to oxygen depletion inside bromeliad tanks, where oxygen (O_2) can drop below micromolar levels within the detrital mass accumulating at the tank bottom (Guimaraes-Souza *et al.*, 2006). This oxygen depletion promotes fermentative activity that can decrease pH to levels below 4 (Goffredi *et al.*, 2011b). Along such strong redox gradients, nitrate (NO_3^-), sulfate (SO_4^{2-}) and eventually carbon dioxide (CO_2) may become alternative terminal electron acceptors for bacterial and archaeal respiration (Canfield and Thamdrup, 2009), potentially causing nitrogen loss via denitrification or driving sulfur cycling and methanogenesis. High concentrations of methanogens and intense methanogenesis have indeed

been detected in bromeliads (Martinson *et al.*, 2010; Goffredi *et al.*, 2011a; Brandt *et al.*, 2016), however the role of other potentially important anaerobic pathways remains unknown. Dissimilatory sulfur and nitrogen metabolism, for example, are typically active in other aquatic sediments and oxygen-depleted water columns, where they strongly shape local physicochemical conditions (Canfield and Thamdrup, 2009). Moreover, the relative roles of various microbial functional groups, including photoautotrophs, chemolithotrophs and heterotrophs, remain largely unknown. For example, while metatranscriptomics provided information on which pathways are active (Goffredi *et al.*, 2015), it is less suited for quantitative comparisons between pathways or between ecosystems because mRNA content correlates poorly with metabolic and biosynthetic rates in natural environments (Moran *et al.*, 2013).

Here we used DNA sequencing and physicochemical measurements to elucidate the structure and potential function of bacterial and archaeal communities in bromeliads from a coastal Brazilian restinga, Jurubatiba National Park (Fig. 1A). By far the most abundant bromeliad species in Jurubatiba are *Aechmea nudicaulis* and *Neoregelia cruenta* in the subfamily *Bromelioideae* (Cogliatti-Carvalho *et al.*, 2001), both of which are tank-forming (type III, sensu Pittendrigh, 1948). *A. nudicaulis* tends to grow in more open areas and, sometimes, on the edge of vegetation patches, and its foliage forms long and narrow tube-shaped tanks (Fig. 1B). In contrast, *N. cruenta* grows preferentially on the edge of vegetation patches and, sometimes, inside the patches, and its foliage is more open and shallow (Fig. 1C). These differences in phenology and location between the two bromeliad species influence the geobiological characteristics in their tanks (Guimaraes-Souza *et al.*, 2006). To assess the generality of our findings within bromeliad species, as well as potential differences across tank (type III) bromeliad species, we considered several individual plants from both species (22 *A. nudicaulis* and 9 *N. cruenta*). We focused on the communities within the detritus deposited at the bottom of the bromeliad tanks, where most of the decomposition and nutrient cycling takes place. To assess the taxonomic composition of the communities, we used DNA amplicon sequencing of the 16S rRNA gene. To estimate the relative abundances of various metabolic functional groups, such as potentially involved in methanogenesis or denitrification, we performed shotgun environmental DNA sequencing (metagenomics) and counted the number of metagenomic sequences associated with each functional group. In a recent study on the same *A. nudicaulis* bromeliads, we observed a remarkably preserved metagenomic functional composition of bacterial and archaeal communities, which contrasted a highly variable taxonomic composition between bromeliads (Louca *et al.*, 2016a). In the present study, we examine this functional composition in detail and discuss its meaning in terms of the biogeochemistry of the bromeliad tank ecosystem. To facilitate the interpretation of metagenomic content, whenever possible, we associated detected taxa with various potential metabolic functions using the existing literature on cultured organisms (Louca *et al.*, 2016b,a). To explore the potential interaction between environmental conditions and functional community structure, we performed correlation analysis using several physicochemical variables, such as tank depth, pH and concentration of dissolved organic carbon (DOC). Many of the considered variables are common limnological variables or are known to affect macroinvertebrate communities and bacterial processes in bromeliads (Haubrich *et al.*, 2009; Marino *et al.*, 2013). Based on our findings, we discuss potential differences between the two bromeliad species as well as between bromeliads and other ecosystems. For the latter comparison, we analysed 16S sequencing data from sediments in eight freshwater lakes and from soil in five different regions around the world.

Results and discussion

Overview of site and bromeliads

At the time of sampling (January 2015) days were mostly sunny, dry and hot, and were preceded by several weeks of drought. A large fraction of bromeliads (notably *N. cruenta*) had completely dried out, hence we chose bromeliads mainly based on the availability of sufficient fluid for chemical and biological sampling. In *A. nudicaulis* bromeliads, their long narrow foliage severely limits the amount of light reaching the fluid surface and the rate of water evaporation, and water content was generally higher than in *N. cruenta*. In *N. cruenta*, coarse litter content was typically higher than in *A. nudicaulis*, to the extent that litter accumulated on top of the tank's fluid contents (Fig. 1C). The detritus at the bottom of all bromeliad tanks was fine and porous (Fig. 1D), while the overlying fluid was mostly clear in *A. nudicaulis* and turbid in *N. cruenta* (Fig. 1O).

Taxonomic composition of microbial communities

Clustering and taxonomic annotation of 16S rRNA sequences revealed rich detrital microbial communities, with 600–800 operational taxonomic units (OTUs, at 99% similarity) detected and taxonomically classified (at the species, genus or some higher level) in each bromeliad. At the OTU level, microbial communities exhibited strong variation in composition across bromeliads. The core microbiome, that is the set of OTUs found in all bromeliads, comprised only 35 OTUs (Supporting Information Fig. S1), and any two bromeliads shared only ~30%–45% of their OTUs. This overlap between communities is significantly lower than would be expected under a null model of random

sequencing of the regional OTU pool ($P < 0.001$, calculated as in Louca *et al.* (2016a)). The low overlap of OTUs found in different bromeliads is consistent with a previously reported high functional redundancy in the regional OTU pool, that is the coexistence at regional scales of OTUs capable of performing similar metabolic functions (Supporting Information Fig. S2 and Louca *et al.*, 2016a). This functional redundancy presumably allows each metabolic niche to be occupied at similar densities in each bromeliad but by alternative microorganisms, while the precise composition within each functional group may be determined by processes other than metabolic niche effects. For example, biotic interactions such as phage-host dynamics or priority effects, have been suggested previously as potential drivers of variation within functional groups, even if the overall functional community structure is constant (Louca *et al.*, 2016a).

All OTUs in the core microbiome were identified as uncultured organisms belonging to a diverse set of clades, such as the family *Chitinophagaceae* (some members of which hydrolyse chitin or cellulose; Chung *et al.* (2012)), the family *Caulobacteraceae* (most members of which are known to form biofilms; Dworkin *et al.* (2014)), the family *Xanthobacteraceae* (many members of which use hydrogen and/or reduced sulfur compounds for energy; Dworkin *et al.* (2014)), the obligately anaerobic family *Ruminococcaceae* (Vos *et al.*, 2011) and the photoheterotrophic genus *Rhodomicrobium* (Ramana *et al.*, 2013). At higher taxonomic levels (e.g. class or phylum level), microbial communities exhibited much greater overlap and similarity in taxon abundances than at the OTU level, suggesting that the environmental conditions in bromeliad tanks may select for particular broad clades but not for specific OTUs within each clade. Most communities were dominated by the classes *Alphaproteobacteria* (notably within the families *Hyphomicrobiaceae*, *Rhodospirillaceae* and *Acetobacteraceae*; Supporting Information Fig. S3) and *Acidobacteria* (notably within the family *Acidobacteriaceae*), followed by members of the Verrucomicrobia OPB35 soil group, the *Methanobacteria* (notably within the family *Methanobacteriaceae*), the *Deltaproteobacteria*, the *Spartobacteria* and the *Betaproteobacteria* (Supporting Information Fig. S4). High relative abundances of *Alphaproteobacteria*, *Acidobacteria* (in *A. nudicaulis*) and *Betaproteobacteria* (in bromeliads *Aechmea mariae-reginae*) have been reported previously for tank water microbial communities (Goffredi *et al.*, 2011b). High transcription activities of *Acidobacteria*, *Alphaproteobacteria*, *Verrucomicrobia*, *Deltaproteobacteria*, *Betaproteobacteria* have been detected in neotropical bromeliad *Werauhia gladioliflora* (Goffredi *et al.*, 2015). Most known *Rhodospirillaceae* are photoheterotrophic in light under anoxic conditions, or chemotrophic in the dark, while all known *Acidobacteriaceae* are chemoheterotrophs (Parte *et al.*, 2011). Most *Acetobacteraceae* ('acetic acid bacteria') are capable of oxidizing ethanol to acetic acid, potentially contributing to the acidification of the bromeliad tank contents (pH $\sim 4.5-5.5$, Fig. 1M). All known *Methanobacteriaceae* archaeal species are strict anaerobes and many obtain their energy via H_2/CO_2 methanogenesis (Dworkin *et al.*, 2014). Indeed, *Methanobacteriaceae* were previously found at high proportions in methane-producing neotropical bromeliads (Martinson *et al.*, 2010; Brandt *et al.*, 2015). In almost all bromeliads we also found archaea of the uncultured Miscellaneous Crenarchaeotic Group. Members of this group are widespread in anoxic eutrophic marine and freshwater sediments worldwide, and are believed to be involved in extracellular anaerobic protein remineralization (Lloyd *et al.*, 2013; Fillol *et al.*, 2015) and, potentially, methanogenesis (Evans *et al.*, 2015). The ubiquity of the above organisms in the bromeliad tanks shapes the picture of microbial communities adapted to an organic-carbon rich, oxygen-limited environment at the tank bottom.

Functional structure of microbial communities

Metagenomic functional profiles (Fig. 2A) as well as functional annotation of OTUs (Fig. 2B) revealed a rich repertoire of metabolic functional groups in bromeliads. Functional community structure was similar across all bromeliads, although functional similarity was highest for bromeliads of the same species. Of the considered functional groups, those associated with fermentation, aerobic respiration and carbon fixation were generally the most abundant, indicating that both heterotrophs as well as autotrophs are important members of bromeliad microbial communities. Moreover, we detected several genes associated with the use of terminal electron acceptors (TEA) other than oxygen for respiration, such as fumarate or inorganic sulfur and nitrogen compounds. We detected much fewer photoautotrophs than heterotrophs, and much fewer genes exclusively associated with photoautotrophy (photosystems I and II) than genes associated with heterotrophy. We note that some of the genes (e.g. *pufM*) potentially involved in anoxygenic photoautotrophy were not counted towards the latter because these genes may also be involved in photoheterotrophy. In principle, this conservative approach may have led to an underestimation of genes potentially involved in photoautotrophy. However, this scenario is unlikely because OTUs known to be anoxygenic photoautotrophs were much more rare than photoheterotrophs (by two orders of magnitude; Fig. 2B). The role of photoautotrophy as an energy source thus appears to be of minor importance to the microbial communities examined here, especially in the detritus-rich and light-deprived bottom of the tanks, in agreement with the conventional view that bromeliad food webs are mainly

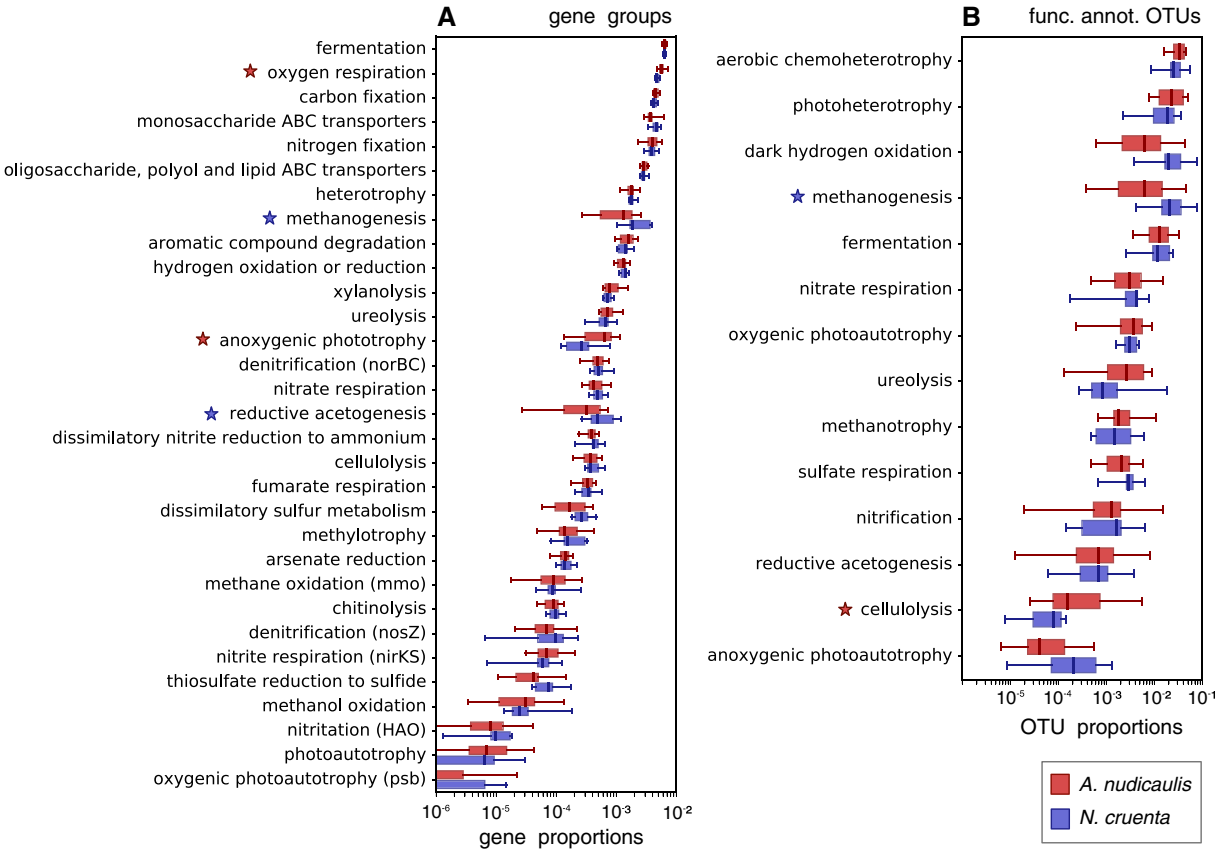

Fig. 2. Relative abundances of functional groups in bromeliads.
A. Box-plots of relative gene abundances based on metagenomic sequences, shown separately for *A. nudicaulis* (red) and *N. cruenta* (blue) (one box per functional group and per bromeliad species). For the list of genes (KEGG orthologs) included in each group, see Supporting Information Table S4. B. Box-plots of relative abundances of OTUs associated with various metabolic functions, used to facilitate the interpretation of gene abundances (one box per functional group and per bromeliad species). In both figures, boxes comprise 50% of the values, and whisker bars comprise 95% of the values, around the median. Red and blue stars indicate groups that were significantly more abundant ($P < 0.05$) in *A. nudicaulis* or *N. cruenta* respectively. Detailed profiles for each bromeliad are provided in Supporting Information Fig. S5. [Colour figure can be viewed at wileyonlinelibrary.com]

detritus-based (Kitching, 2001; Guimaraes-Souza *et al.*, 2006; Bouard *et al.*, 2012).

The high concentration of coarse detrital material (e.g. decomposing leaves, personal observation) and dissolved organic carbon inside the bromeliad tanks (26 $mg \cdot L^{-1}$ in *N. cruenta* and 89 $mg \cdot L^{-1}$ in *A. nudicaulis*) support a plethora of catabolic pathways for the degradation of complex organic molecules. Genes associated with fermentation, monosaccharide transport or heterotrophy were among the most abundant gene groups considered (Fig. 2A). Likewise, taxa associated with aerobic chemoheterotrophy and fermentation constituted a substantial fraction of functionally annotated OTUs, both in terms of total abundances (Fig. 2B) and in terms of OTU richness (Supporting Information Fig. S2). Genes coding for bacterial and archaeal chitinases, cellulases (endoglucanases and cellobiosidase) and xylanases (*xynAB*) were detected in all bromeliads. Hence, chitin, an important component of arthropod exoskeletons, as well as cellulose and xylans, both important components of plant cell walls, appear to sustain active chitin, cellulose and xylan hydrolysis in these environments, supporting previous analogous suggestions (Goffredi *et al.*, 2011b).

In all bromeliads, we detected several genes potentially involved in the respiration of nitrogen compounds, including all denitrification steps (nitrate reductase *narGHIJ*, periplasmic nitrate reductases *napAB*, nitrite reductase *nirK*, nitric oxide reductase *norBC* and nitrous-oxide reductase *nosZ*) and dissimilatory nitrite reduction to ammonium ('ammonification'; nitrite reductase *nirBD* and *nrfA*). In 25 out of 31 bromeliads we also detected genes potentially involved in aerobic ammonia oxidation to nitrite (hydroxylamine dehydrogenase *hao*), which is the first step in the nitrification pathway. Further, all bromeliads contained genes associated with ureolysis (ureases), an ammonia-producing precursor to nitrification. Both nitrification and

ureolysis are important contributors to nitrogen cycling in larger aquatic and terrestrial ecosystems (Canfield *et al*., 2010). The presence of putative urea hydrolysers, nitrifiers and denitrifiers (but not ammonifiers) was confirmed by functional annotation of OTUs in almost all bromeliads (Fig. 2B). We did not detect any OTUs known to perform anaerobic ammonia oxidation (anammox), a common pathway in other anoxic environments (Canfield *et al*., 2010), although we detected several uncultured *Planctomycetales* potentially capable of anammox (Dalsgaard *et al*., 2005). The distribution of anammox across microbial clades is still poorly understood, and hence at this point we cannot rule out anammox activity in bromeliads. Bromeliads contained at most trace amounts of nitrous oxide ($< 10\,nM\,N_2O$, Fig. 1W). Given the ubiquity of *nosZ* genes, representing the final denitrification step that converts nitrous oxide to N_2, it appears that denitrification is nearly complete and that little of the respired nitrogen escapes as intermediate nitrous oxide into the atmosphere. Overall, our findings suggest that bromeliad tanks exhibit intense nitrogen cycling and, in particular, loss of fixed nitrogen via dissimilatory reduction of nitrogen compounds to N_2. The loss of fixed nitrogen as gaseous N_2 through denitrification is known to affect primary productivity in the ocean (Canfield *et al*., 2010). In bromeliads, intense remineralization of allochthonous organic matter as well as potentially nitrogen input from animal excretions and carcasses (Romero *et al*., 2006) may counteract denitrification and provide sufficient nitrogen for assimilation; indeed, we found high nitrogen concentrations in the tank water of most bromeliads ($\sim$50–100 μM total N; Supporting Information Fig. 1S). These nitrogen concentrations are comparable to those typically found in eutrophic lakes (Wetzel, 2001). In a previous survey of *N. cruenta* with much lower nitrogen concentrations (median $NH_4^+ + NO_3^- \sim 19.4\,\mu M$), no clear bottom-up limiting factor on bacterial growth was found and ammonium concentration only explained 8.9% of the variance (Haubrich *et al*., 2009). Hence, in bromeliads with high litter and nitrogen content, as observed here, nitrogen may not be a limiting factor to microbial productivity, although this prediction may depend on the organism at hand and enrichment experiments are needed for definite conclusions (Ngai and Srivastava, 2006).

In all bromeliads we found genes associated with nitrogen fixation (nitrogenase *nifDHK* and *anfG*), consistent with previous findings of nitrogenase genes in rainforest bromeliad tanks (Goffredi *et al*., 2011b). Accordingly, we found several OTUs potentially capable of nitrogen fixation (4% mean relative abundance), for example in the Alphaproteobacterial genera *Azospirillum* and *Methylocystis* (Garrity, 2005). This suggests that despite the high concentration of fixed nitrogen and intense nitrogen cycling, energetically costly nitrogen fixation may still be performed. Alternatively, the ability for nitrogen fixation may be present but inactive. The latter scenario appears more likely, because measured molar N:P ratios ($\sim$25−30, Fig. 1U) are higher than average N:P ratios in marine and freshwater lake water columns and sediments ($\sim$20; Sardans *et al*., 2011). These high N:P ratios likely result from the remineralization of incoming litter such as leaves, which typically exhibit average N:P ratios in the range 28–30 (Sardans *et al*., 2011), but might also result from a preferential uptake of phosphorous by the plants themselves (Zotz and Asshoff, 2010). While most N:P ratios ($\sim$29 on average) found here are greater than previously reported threshold N:P ratios, above which bacteria became P-limited in freshwater lakes ($\sim$22; Elser *et al*., 1995), total P concentrations themselves were also generally high ($\sim 2-4\,\mu M$) and comparable to eutrophic lakes (Wetzel, 2001). Hence, it is possible that neither N nor P were important limiting factors to overall bacterial and archaeal productivity in the bottom detritus, and that energetic constraints – linked to TEA availability – may have been more important.

Bromeliads contained several genes associated with dissimilatory sulfur metabolism, such as genes coding for sulfite reductases *dsrAB*, adenylylsulfate reductases *aprAB* and thiosulfate reductases *phsAC*. The mere detection of *dsrAB* and *aprAB* genes does not clarify the direction in which the corresponding enzymes act, because different variants of these genes can act as reductases or oxidases. *phsAC* has so far only been associated with thiosulfate reduction to sulfide (Hinsley and Berks, 2002), and we did not detect any genes of the *sox* sulfur oxidation system in 30 out of 31 bromeliads. Functional annotation of OTUs revealed 10–100 fold higher abundances of known sulfate respires compared to known oxidizers of reduced sulfur compounds (either for chemolithotrophy or anoxygenic photoautotrophy), suggesting that most of the dissimilatory sulfur metabolism may be reductive. Measured hydrogen sulfide concentrations were below the detection limit in all bromeliads ($<$20 nM), suggesting either that sulfide produced from sulfate reduction is rapidly oxidized or that sulfate reduction does not proceed all the way to sulfide. The latter explanation appears less likely, because *aprBA* genes and *dsrAB* genes exhibited similar relative abundances (on average $\sim$0.01 % of all annotated sequences). Hence, complete 'cryptic' sulfur cycling between sulfate and sulfide – perhaps enabled by reaction of sulfide with iron oxides – may have taken place in the bromeliads, but we may have failed to identify the majority of sulfide oxidizing organisms.

We also found high abundances of genes associated with methanogenesis (methyl-coenzyme M reductase *mcrABCDG* and heterodisulfide reductase *hdrABC*), as well as high abundances of methanogenic archaea (e.g. *Methanomicrobiales*, *Methanobacteriales*, *Methanosarcinales* and *Methanocellales*; on average 16% among functionally

classified OTUs), consistent with similar findings in bromeliads in neotropical forests (Martinson *et al.*, 2010; Goffredi *et al.*, 2011a; Brandt *et al.*, 2016). Genes associated with hydrogen oxidoreduction (e.g. ferredoxin hydrogenase) were comparable in abundance to methanogenic genes, and some of the detected methanogens (e.g. one *Methanobacterium* sp.; Garrity, 2001) belonged to taxa known to oxidize hydrogen with carbon dioxide ($CO_2 + 4H_2 \rightarrow CH_4 + 2H_2O$). This suggests that methanogenesis was partly driven by hydrogen. At least one detected OTU (present in 16 out of 31 bromeliads) belonged to a genus so far known to comprise exclusively acetoclastic methanogens (*Methanosaeta* sp.; Garrity, 2001). Acetoclastic methanogenesis ($CH_3COOH \rightarrow CH_4 + CO_2$) may thus have also been active, perhaps acting as a sink for acetate produced by fermentation. Furthermore, the detection of genes coding for acetyl-CoA decarbonylase (*cdhABCDE*; Fig. 2A) and of putative reductive acetogens in several bromeliads (Fig. 2B) suggests that reductive acetogenesis ($2CO_2 + 4H_2 \rightarrow CH_3COOH + 2H_2O$) may be competing with hydrogenotrophic methanogenesis for hydrogen. Genes and OTUs associated with methanogenesis were much more abundant than genes and OTUs associated with sulfate respiration (Fig. 2). This suggests that sulfate may be severely depleted in these organic carbon-rich environments and is quickly replaced by CO_2 as a TEA. An extreme sulfate limitation would explain the appearance of a methanic zone in these shallow systems (Capone and Kiene, 1988).

We found putative methanotrophs in all bromeliads (~1%–3% of functionally classified OTUs) as well as methane monooxygenase (*mmo*) genes in almost all bromeliads. Methanogenesis thus appears to provide a niche for methane (CH_4) oxidation in bromeliad detritus, consistent with previous reports of active methanotrophic bacteria in another bromeliad species, *W. gladioliflora* (Brandt *et al.*, 2016). The accumulation of methane in the tank water (Fig. 1V) indicates that a mismatch exists between methane production and consumption despite the presence of methanotrophs, and that a substantial fraction of the methane produced escapes into the atmosphere before it has had a chance to be re-oxidized. High methane emissions from bromeliad tanks have been found previously (Martinson *et al.*, 2010; Goffredi *et al.*, 2011a). In typical marine and freshwater lake sediments much of the methane produced at depth is re-oxidized in sulfate-methane transition zones before reaching the water column (Hinrichs and Boetius, 2003). A lack of sufficient sulfate for complete methane oxidation, as discussed earlier, would explain the net flux of methane out of bromeliads. Measurements of sulfate concentrations and methane depth profiles in bromeliad tanks are needed to verify this conclusion.

We detected genes associated with anoxygenic phototrophy (e.g. *pufM*), either anoxygenic photosynthesis or photoheterotrophy, in all bromeliads at substantial relative abundances (Fig. 2A). Functional annotation of OTUs verified the presence of anoxygenic photoautotrophs (predominantly *Rhodoplanes* spp.) at low abundances in almost all bromeliads, as well as the presence of photoheterotrophs in all bromeliads at high abundances (24% mean relative abundance) that surpassed those of oxygenic and anoxygenic photoautotrophs combined (3.8% mean relative abundance; Fig. 2B). Photoheterotrophs obtain part or all of their energy from light while avoiding costly CO_2 fixation by actively acquiring reduced carbon from their environment, and typically thrive in stratified lakes or waste lagoons (Madigan and Jung, 2009). Their ubiquity in the bromeliads suggests that the high organic carbon densities allow photoheterotrophs to compete with TEA-limited chemoheterotrophs for carbon and as well as with – potentially light-limited – photoautotrophs. Anoxygenic photoautotrophs, on the other hand, use inorganic electron donors, such as H_2S or H_2, for light-powered carbon fixation (Bryant and Frigaard, 2006). In bromeliad tanks these compounds might be produced in the dark anaerobic bottom through sulfate respiration and fermentation, respectively. Sulfide-consuming anoxygenic photosynthesis, in particular, may partly contribute to maintaining bromeliad tanks free of H_2S and thus habitable for other organisms such as protists and invertebrates. At this point it is unclear whether reduced iron, perhaps produced via iron respiration coupled to sulfide oxidation, also serves as an electron donor for anoxygenic photosynthesis. While we detected *Rhizomicrobium electricum*, a known iron and fumarate respirer (Kodama and Watanabe, 2011), at low densities in almost all bromeliads, none of the identified anoxygenic photoautotrophs are known to oxidize iron. High abundances of anoxygenic phototroph-specific *pufM* genes, affiliated with purple non-sulfur bacteria and purple sulfur bacteria, were found previously and concurrently with high bacteriochlorophyll a concentrations in several bromeliads (including two *Aechmea* species; Lehours *et al.* (2016)). Photoheterotrophs or, more generally, anoxygenic phototrophs thus appear to be widespread and important functional groups in bromeliad tanks.

We note that some of the functionally annotated OTUs (Fig. 2B) belonged to clades known to perform multiple metabolic functions (see Supporting Information Fig. S6), and it is unclear which of the functions were actually active at the time of sampling. For example, the only identified iron respiring bacterium, *R. electricum*, is also capable of fumarate, nitrate and oxygen respiration (Kodama and Watanabe, 2011), and hence it is unknown whether iron respiration is actually occurring inside bromeliad tanks. Metatranscriptomics, metaproteomics or in-situ rate measurements (Martinson *et al.*, 2010) are needed to verify the biochemical processes suggested by DNA sequencing. Furthermore, the microbial communities described here represent 'composite' communities spanning multiple redox zones, because we extracted DNA after mixing the

entire detrital material. In situ, various metabolic pathways (e.g. using different TEAs) most likely display a depth partitioning similar to that found in other freshwater anoxic sediments (Capone and Kiene, 1988; Canfield and Thamdrup, 2009). Depth-resolved molecular sampling and chemical profiling (Guimaraes-Souza *et al.*, 2006) would thus greatly enhance our understanding of bromeliad tank biogeochemistry.

Relating functional community structure to environmental conditions

To assess the potential effects of individual environmental conditions on community function and vice versa, we calculated Spearman rank correlations between the relative abundances of metagenomic functional groups and several environmental variables. We considered common limnological variables such as pH, salinity, total N and P concentrations, as well as other potentially important variables such as canopy coverage, detrital volume (volume of slurry-like compartment) and methane concentrations (Fig. 1E–X). We found that, across all bromeliads, functional groups were most correlated with detrital volume, methane concentrations, turbidity, water colour (light absorption at 440 nm) and canopy coverage, while the types of correlations (positive or negative) were similar for all five of these variables (Fig. 3). These variables correlated positively with genes for methanogenesis, reductive acetogenesis, cellulolysis, hydrogen oxidation or reduction, denitrification (*norBC*), thiosulfate reduction to sulfide and xylanolysis, and correlated negatively with genes involved in fermentation, oxygen respiration, anoxygenic phototrophy, aromatic compound degradation and ureolysis. Functional groups also correlated with plant height, tank volume (bottom to water surface) and dissolved organic carbon, albeit to a lesser extent (Fig. 3). Most of the significant correlations remained significant and similarly strong when we controlled for bromeliad species (by considering only *A. nudicaulis*; Supporting Information Fig. S9), although plant height and tank volume were notable exceptions (see discussion below). The fact that most correlations were similar across both bromeliad species as within a single species, suggests that differences in microbial community function are driven by the environmental characteristics of the bromeliads rather than by bromeliad species identity per se, consistent with similar observations made for invertebrate communities (Marino *et al.*, 2013).

The strong correlation of detrital volume with several functional groups suggests that the size of the detrital compartment influences the stratigraphy at depth, and thus affects the relative importance of metabolic pathways and TEAs used for carbon catabolism. Indeed, detrital volume correlated strongly positively with methane concentrations (Supporting Information Fig. S7). The fact that functional groups correlated less with tank depth and tank volume than with detrital volume, calls for an explanation. Redox gradients are generally much more compressed in aquatic sediments – and presumably in bromeliad detritus – than in water columns (Capone and Kiene, 1988), mostly due to slower ion diffusion rates and greater decomposition rates in the former (Iversen and Jørgensen, 1993). As a result, detrital volume is expected to have stronger influence than water volume on TEA supply, and hence on metabolic processes. Previous studies in epiphytic bromeliads revealed a positive correlation between methane production and tank diameter (Martinson *et al.*, 2010), as well as between methanogen abundances and plant height (Goffredi *et al.*, 2011a), but neither study explicitly considered the volume of the detritus within the tanks. Our results suggest that methanogenesis may be more strongly influenced by the detrital volume, rather than by overall plant or tank size *per se*.

The strong correlation between canopy coverage and several functional groups is consistent with previous studies, which showed a strong correlation between canopy coverage and the relative importance of autotrophy vs. detritivory in bromeliad tanks (Bouard *et al.*, 2012; Farjalla *et al.*, 2016). As discussed above, based on our sequencing data photosynthesis likely played a minor role in the bromeliads compared to detritivory, especially in *A. nudicaulis* whose tank interior had little exposure to direct sunlight. It thus appears likely that canopy coverage affected community function through the amount (and perhaps type) of litter entering the tank, rather than through the modulation of light exposure. This interpretation is supported by the fact that canopy coverage correlated significantly positively with detrital volume (Supporting Information Figs. S7 and S8), and the fact that most functional groups correlated similarly with detrital volume as they did with canopy coverage (Fig. 3 and Supporting Information Fig. S9).

None of the considered functional groups correlated significantly with pH. The weak correlation of pH with functional community structure appears in contrast to previous experiments that showed strong pH-induced shifts in the taxonomic composition of microbial communities in bromeliad tank water (Goffredi *et al.*, 2011b). Our results suggest that factors related to energetic constraints (TEA availability) and the associated metabolic niche structure, are more important than pH in shaping microbial community function in the bottom detritus.

We emphasize that care must be taken when inferring causal relationships purely based on correlation studies such as ours. For example, water properties such as turbidity and nutrient contents, are likely to influence and be influenced by microbial communities. Likewise, methane concentration should be regarded as a proxy, rather

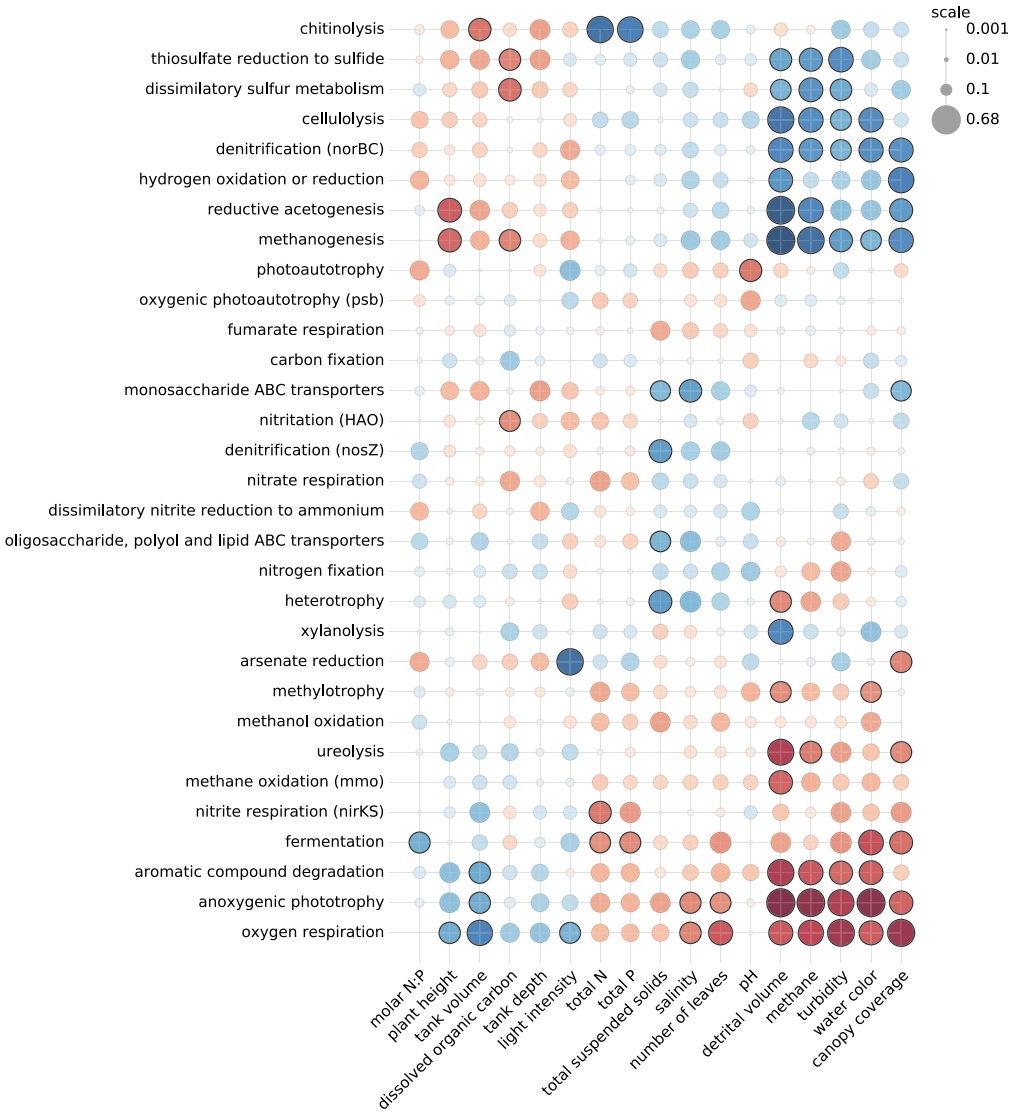

Fig. 3. Metagenomic functional groups vs. environmental variables across bromeliads. Spearman rank correlations between relative metagenomic functional group abundances (rows) and environmental variables (columns) across all bromeliads. Blue and red colors correspond to positive and negative correlations respectively. Circle size and color saturation are proportional to the magnitude of the correlation. Statistically significant correlations ($P < 0.05$) are indicated by black perimeters. Rows and columns are hierarchically clustered by similarity. For correlations within a single bromeliad species (*A. nudicaulis*) see Fig. S9. [Colour figure can be viewed at wileyonlinelibrary.com]

than a cause, of methanogenesis; in fact, our results reveal methane as an important chemical proxy of overall microbial functional community structure. We also note that significant correlations between functional groups and certain environmental variables – notably plant height – may result from a correlation of these variables with other variables that more directly influence community function (Supporting Information Fig. S7). In fact, plant height and several other variables differ systematically between bromeliad species (Fig. 1H), and when we controlled for bromeliad species plant height was no longer significantly correlated with any functional group (Supporting Information Fig. S9).

Microbial community differences between A. nudicaulis *and* N. cruenta

To assess the extent to which microbial community structure differed between bromeliad species, we performed permutational multivariate analysis of variance (PERMANOVA; Anderson and Walsh, 2013), based on pairwise Bray-Curtis dissimilarities (Legendre and Legendre, 1998)

of taxonomic as well as metagenomic composition. PERMANOVA revealed that the two bromeliad species exhibited significantly different microbial communities at all taxonomic levels (OTU, genus, family etc., $P < 0.05$) as well as in terms of their metagenomic profiles (overview in Table S1). In addition, permutation tests revealed that the relative abundances of about 18% of OTUs differed significantly ($P < 0.05$) between the two bromeliad species. This fraction is much higher than the false detection rate (5%) expected under the null hypothesis of perfectly equivalent bromeliad species, indicating that several organisms may be better adapted to certain bromeliad species. The fraction of taxa exhibiting significantly different abundances between bromeliad species gradually decreased at higher taxonomic levels (Supporting Information Table S1 and Figs. S3, S4, S10 and S11).

Previous bacterial taxonomic community profiling using 16S rRNA DGGE failed to detect any association between bromeliad species and DGGE profiles (Farjalla *et al*., 2012). These findings suggested that physicochemical differences between the two bromeliad species would not be strong enough to cause detectable systematic shifts in bacterial community structure. Instead, our results suggest that previous DGGE-based profiling methods may have been too coarse to detect systematic differences between bromeliad species, especially since these differences seem to be most pronounced at lower – and thus harder to resolve – taxonomic levels (e.g. OTU and genus level). Indeed, DGGE can fail to differentiate between bacterial species (Kisand and Wikner, 2003), and other studies have shown differences between bromeliad species both in terms of microbial community composition as well as metabolism (Martinson *et al*., 2010; Goffredi *et al*., 2011b).

Only 13% of metagenomic functional groups (as listed in Fig. 2A) and 16% of KEGG gene orthologous groups (KOGs; Kanehisa and Goto, 2000) exhibited significantly different relative abundances between bromeliad species (Table S1). When we combined KOGs into standard categories of the KEGG ontology, 51% of level-B categories and 23% of level-C categories exhibited significantly different abundances between bromeliad species, although their mean relative abundances remained very similar in both bromeliad species (relative differences were typically less than 10%). Genes for anoxygenic phototrophy ($P = 0.028$) and oxygen respiration ($P < 0.001$) had significantly higher relative abundances in *A. nudicaulis* (about 1.9× and 1.2× higher than in *N. cruenta*, respectively; Fig. 2A). Genes associated with methanogenesis ($P = 0.008$) and reductive acetogenesis ($P = 0.032$) had higher relative abundances in *N. cruenta* (about 1.9× and 1.8× higher than in *A. nudicaulis*, respectively; Fig. 2A), suggesting a shift towards the use of CO_2 as a TEA. This observation is consistent with elevated methane concentrations (Fig. 1V) and significantly higher relative abundances of known methanogens in *N. cruenta* bromeliads ($P = 0.049$, Fig. 2B). Methanogenesis and reductive acetogenesis correlated strongly positively with detrital volume and canopy coverage (even within a single bromeliad species; Fig. 3 and Supporting Information Fig. S9), both of which tend to be greater in *N. cruenta* (Fig. 1). Furthermore, *N. cruenta* tanks were generally more loaded with plant litter, in part because *N. cruenta* grew preferentially in more densely vegetated areas and because *N. cruenta* foliage is more open than *A. nudicaulis* foliage (Figs. 1B and C). The greater accumulation of litter in *N. cruenta* may be limiting the intrusion of TEAs (especially oxygen) in addition to increasing overall oxidant demand, resulting in elevated methanogenesis within the detritus (Capone and Kiene, 1988).

Microbial community differences between bromeliads and other freshwater sediments

To compare the microbial communities found in the bromeliads to those in other freshwater or soil environments, we analysed 16S amplicon sequences from sediments in eight freshwater lakes and soil from five regions, distributed around the world (Canada, USA, Brazil, Kenya and the Tibetan Plateau; overview in Table S2). We considered samples taken from the surface sediment layer (upper 0–22 cm) or the soil surface (upper 0–20 cm). Sequence data were either generated by us, or obtained from the Earth Microbiome Project (Gilbert *et al*., 2014). We compared the taxonomic composition of microbial communities as well as their estimated functional potential (based on a functional classification of OTUs) between bromeliads, lake sediments and soil similarly to our previous comparisons between bromeliad species. PERMANOVA of Bray-Curtis dissimilarities revealed stark differences in taxonomic community composition between bromeliads and lake sediments as well as between bromeliads and soil, at all taxonomic levels ($P < 0.001$). These differences were stronger than the differences between the two bromeliad species (Fig. 4A). Moreover, permutation tests for individual taxa revealed that a high fraction of taxa occurred significantly ($P < 0.05$) more frequently in bromeliads than in lake sediments, or vice versa (e.g. ∼34% of genera and ∼39% of families, overview in Table S3). A similarly high fraction of taxa occurred significantly more frequently in bromeliads than in soil, or vice versa (e.g. ∼39% of genera and ∼44% of families). These differences between bromeliads and lake sediments or between bromeliads and soil, are likely largely driven by the particular geochemical features of these environments.

Comparison of functionally classified OTUs showed clear differences in functional group proportions, with 6 out of 15 functional groups having significantly ($P < 0.05$)

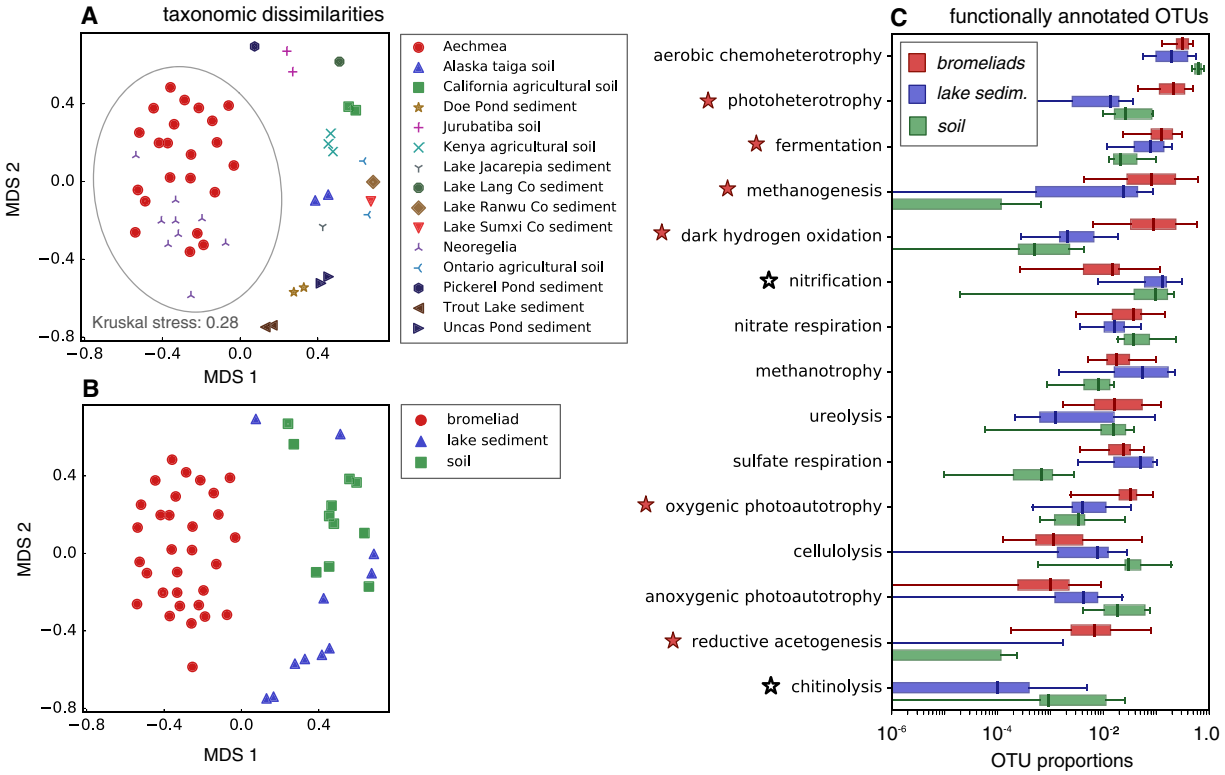

Fig. 4. Comparing microbial communities between bromeliads, lake sediments and soil.
A. Metric multidimensional Scaling (MDS) plot of Bray-Curtis taxonomic dissimilarities (genus level) between microbial communities in bromeliads, freshwater lake sediments and soil (one point per sample). Points closer to each other correspond to more similar microbial communities. Bromeliad samples are circled.
B. Same as (A), but with samples grouped as 'bromeliad', 'lake sediment' and 'soil' for easier identification.
C. Box-plots of relative abundances of OTUs associated with various metabolic functions, shown separately for bromeliads (red), freshwater lake sediments (blue) and soil (green) (one box per functional group and per environment type). Boxes comprise 50% of the values, and whisker bars comprise 95% of the values, around the median. Filled (or empty) stars indicate functional groups that had significantly ($P < 0.05$) higher (or lower) relative abundances in bromeliads than in lake sediments and than in soil. [Colour figure can be viewed at wileyonlinelibrary.com]

higher relative abundances in bromeliads compared to lake sediments and compared to soil (based on permutation tests; Fig. 4C). Notably, OTUs classified as photoheterotrophs, methanogens and reductive acetogens had significantly higher proportions in bromeliads than in the other two environments, supporting our previous conclusions that CO_2 respirers and photoheterotrophs are important and characteristic metabolic functional groups in the bromeliad tank ecosystem. The proportion of OTUs classified as nitrate respirers in bromeliads was similar to those in soil, but significantly higher than in lake sediments. OTUs classified as nitrifiers or as chitin degraders were significantly underrepresented in bromeliads, compared to lake sediments or soil. We note that here we only considered surface sediments and surface soil. It is possible that bromeliad microbial communities would exhibit greater similarities with deeper layers in freshwater lake sediments or soil, where CO_2 respiration and methanogenesis usually become more important (Capone and Kiene, 1988; Serrano-Silva *et al.*, 2014).

Conclusions

Our findings provide evidence for strong fermentative activity and the use of several alternative TEAs to oxygen within bromeliad tanks, consistent with oxygen-limited conditions and high organic carbon content. The detection of genes and OTUs potentially involved in dissimilatory sulfur, nitrogen, hydrogen and carbon cycling shapes the picture of a complex and distributed metabolic network that involves stepwise electron transport across a cascade of electron acceptors (Canfield and Thamdrup, 2009). This metabolic network drives the remineralization of mostly allochthonous organic material, and its performance may ultimately be limited by the diffusive transport of electron acceptors across the tank's contents (depth profile data are needed to verify this prediction). A limitation of detrital decomposition rates by TEA availability is consistent with recent findings, that the relative importance of autochthonous vs. allochthonous carbon sources for invertebrates in bromeliad tanks was not influenced by detrital density (Farjalla *et al.*, 2016). Sulfate was likely strongly limiting as

an electron acceptor in the bromeliads examined here, to the extent that the methanic zone largely displaced the sulfidic zone and methanogens exhibited much greater abundances than sulfate respirers. Greater detrital content, as observed particularly in *N. cruenta*, was associated with a greater importance of methanogenesis and methanogenesis-associated pathways. Anoxygenic phototrophs, notably photoheterotrophs, constituted an important part of the bacterial and archaeal communities in the detritus and largely outnumbered oxygenic photoautotrophs. This challenges the conventional view that chemoheterotrophy and oxygenic photosynthesis constitute the main energy sources for bromeliad tank food webs (Bouard *et al.*, 2012). We emphasize that our conclusions about potential community function are solely based on the relative abundances of detected genes and OTUs associated with various metabolic functions. Gene expression data and/or flux rate measurements are needed to confirm our predictions.

Overall bacterial and archaeal community structure differed significantly between the two bromeliad species, *A. nudicaulis* and *N. cruenta*, both in terms of taxonomic and functional composition. These differences were likely driven by environmental characteristics specific to each bromeliad species (Guimaraes-Souza *et al.*, 2006; Marino *et al.*, 2013). Nevertheless, the majority of metagenomic functional groups (26 out of the 30 considered) was not significantly overrepresented in any of the two bromeliad species. This suggests that while detectable differences existed, the overall biogeochemistry of these aquatic environments was mostly determined by their shared properties such as the accumulation of leaf litter from surrounding trees, low penetration of light to the detritus at the bottom, intense water stagnation, sulfate and oxygen limitation, as well as hot climatic conditions. In contrast, we found much stronger differences between microbial communities in bromeliads and those in freshwater lake sediments or soil from around the world, highlighting the distinct nature of the bromeliad tank ecosystem. We expect most of our findings to also apply to other tank (type III, Pittendrigh, 1948) bromeliads, especially those exhibiting high detrital content. Our work provides a firm baseline towards a mechanistic understanding of the biogeochemistry of these fascinating miniature ecosystems.

Methods

Biological sample collection

All samples were collected from an area of less than 0.2 km^2 in the Jurubatiba National Park, during the period of January 8–10, 2015. We note that a subset of the samples (*A. nudicaulis* bromeliads) was also used in a previous study (Louca *et al.*, 2016a). The overlying water was removed from the bromeliad's central tank using a sterile serological pipette. The remaining detritus was then retrieved using a sterile syringe and a metal spatula, after cut-opening the bromeliad for easier access. The entire detrital content of a bromeliad was retrieved and mixed for sampling. In *A. nudicaulis* the overlying water made up the largest proportion of tank contents (both in terms of volume as well as depth), and in all bromeliads the detrital depth was typically in the range of 2–5 cm. All samples were flash-frozen in liquid nitrogen within 10 min of collection and then frozen in the laboratory at −80°C until further processing. Samples were concentrated via centrifugation (40 000 g for 15 min, balanced using miliQ filtered water) and removal of the overlying water, and then freeze-dried for 24 h. Dried samples were shipped for further processing to the University of British Columbia, Canada, at room temperature in Falcon™ centrifuge tubes.

Chemical analysis of bromeliad tank water

The water on top of the detritus was collected using a serological pipette, stored in 25 mL centrifuge tubes on regular ice in the field and at −4°C in the lab until further analysis (within less than 2 days). Total phosphorus concentrations were determined as the inorganic phosphorus obtained after a procedure of acid-digestion and autoclaving of the water samples and the ascorbic acid-molybdate reaction (Golterman *et al.*, 1978). Total nitrogen concentrations were determined as the concentration of nitrite plus the concentration of nitrate obtained after an acid digestion procedure and autoclavation. Nitrate was transformed into nitrite with a cadmium column via a reduction step, and nitrite was subsequently quantified using a Flow Injection Analysis System (FIA-Asia Ismatec™) (Zagatto *et al.*, 1980), yielding total nitrogen.

Water samples for CH_4 measurement were taken separately (1.5 mL per measurement) and directly from the bromeliad, fixed using formalin (4%) in 3 mL glass vials, kept on regular ice in the field and at 4°C in the lab until analysis within 2 days. Air was sampled from the headspace using a syringe after shaking the vials for 1 min, and headspace CH_4 content was determined using a Shimadzu™ GC-2010AF gas chromatograph equipped with a Rt-QPLOT column (3 m × 0.32 m) and a flame ionization detector (FID-2010). Temperatures of the injection, column and detection were 120, 85 and 220°C respectively. Nitrogen (N_2) was used as the carrier gas.

Conductivity, pH, temperature and Total Suspended Solids (TSS) were measured in the field using an ExStik II EC500™ (ExTech Instruments). Salinity was calculated from conductivity and temperature using the empirical formula reported by Fofonoff and Millard-Junior (1983). Water turbidity was measured in the field using a Hanna Turbidimeter HI98703. For several bromeliads the available water was insufficient for performing some of the above chemical assays. These water samples were diluted in the field using deionized water prior to measuring conductivity, pH, TSS and turbidity. The conductivity, salinity, TSS and turbidity were then corrected using the known dilution factor. The pH of diluted samples was corrected using a standard curve constructed by serial dilution of water from bromeliad B15.

Dissolved organic carbon (DOC) concentrations were determined using by Pt-catalyzed high-temperature combustion with a Shimadzu TOC-VCPN Total Carbon Analyzer™, after filtering through 0.7 μm Whatman™ GF/F glass fibre filters.

Absorption spectra were measured using a Varian 50 Bio UV-Visible Spectrophotometer™, following the manufacturer's procedures. For several bromeliads the available water was insufficient for measuring DOC concentrations and absorption spectra. These water samples were diluted in the lab using deionized water as needed. All measurements were subsequently corrected for the effects of dilution.

Hydrogen sulfide (H_2S) concentration was measured using a Unisense™ Picoammeter PA2000 with a Unisense H_2S-500 electrode, at 2 cm distance from the tank bottom. In all bromeliads, H_2S concentrations were below detection limit ($<$20 nM), and hence these data were not suitable for further analysis. Oxygen concentration was measured using a Unisense™ Picoammeter PA2000 with a Unisense OX-500 electrode, at 2 cm distance from the tank bottom. We note that oxygen concentration and temperature were measured at a different time for each bromeliad, and bromeliad tanks may have exhibited significant temporal variation in oxygen content and temperature throughout the day.

Measurement of other abiotic factors

Light intensity (flux of photosynthetically active radiation) on bromeliads was measured using an LI-250A Lightmeter™ (LI-COR Biosciences), equipped with a US-SQS/L™ spherical micro quantum sensor (Heinz Walz GmbH). The lightmeter was placed on the ground next to the bromeliad at noon (January 10, 2015), after having cut the upper part of the bromeliad to avoid shading of the device by the bromeliad itself. The detrital volume was measured using the tube's scale after allowing for precipitation for 5 min, performing the read at the interface between the precipitated detritus and the overlying transparent water. The total volume of the tank was defined as the total volume of all retrieved fluids (detritus and water). The fluid depth was either measured using a metal wire with engraved cm-scale or using the serological pipette's scale. The latter was transformed to depths upon calibration. Canopy coverage above bromeliads was measured by taking a photo from the top of a bromeliad 'face-up' on a sunny day, and processing the photo using ImageJ™ for contrasting objects against a blue sky background.

16S sequencing

DNA was extracted from the re-hydrated samples using the MoBio PowerSoil® DNA extraction kit, by applying the manufacturer's suggested protocol. Amplification of the 16S rRNA gene was done using universal primers covering the V4 region (*Escherichia coli* 515F: 5′ GTGCCAGCMGCCGCGGTAA 3′ and 806R: 5′ GGACTACHVGGGTWTCTAAT 3′), obtained from the Earth Microbiome Project (Gilbert *et al.*, 2014). The primers included 12-base Golay barcodes that were filtered to reduce primer dimers, as well as Illumina adapters for subsequent sequencing. Amplification was done using the official Earth Microbiome Project 16S amplification protocol version 4_13 (Caporaso *et al.*, 2012). Specifically, amplification was performed in a 25 μL reaction volume and consisting of 13 μL nuclease free water, 10 μL 5Prime Hot Start Taq master mix, 0.5 μL forward primer, 0.5 μL reverse primer, 1 μL template. PCR was performed using an Eppendorf Mastercycler® nexus eco thermocycler. The thermal cycle was set to 3 min at 94°C for initial denaturation, followed by 25 cycles of 45 s at 94°C for denaturation, 60 s at 50°C for annealing and 90 s at 72°C for extension, and followed by 10 min at 72°C for the final extension. Amplicon DNA was quantified with a Qubit® 2.0 fluorometer using the manufacturer's protocol. Amplicon DNA from all bromeliads was combined into a single library, at such proportions that each sample contributed a similar amount of DNA. Primer dimers and residual PCR enzymes were removed from the library using the MoBio® UltraClean PCR Clean-Up Kit. Library quantitation was done by Genoseq Core (University of California, Los Angeles) using a high-sensitivity Agilent Bioanalyzer™ and Kappa Biosystems' Illumina Genome Analyzer™ (KAPA SYBR FAST Roche LightCycler 480) kit, followed by qPCR. Sequencing was done by Genoseq Core using an Illumina MiSeq™ next generation sequencer by applying the manufacturer's standard protocol.

Sequencing yielded a total of 3 813 462 paired-end 16S rDNA amplicon sequences (2 $\times$ 300 base pairs each). Sequence analysis was performed using the QIIME toolbox (Caporaso *et al.*, 2010). Paired-end reads were merged after trimming forward reads at length 240 and reverse reads at length 160. Merged sequences were quality filtered using QIIME's default settings, yielding 3 508 476 sequences of median length 253. Remaining sequences were error-filtered and clustered de-novo using cd-hit-otu (Li *et al.*, 2012) at a 99% similarity threshold, generating 2113 OTUs representing 2 729 382 sequences across all samples. Sample B17 yielded by far the fewest sequences (5811 sequences corresponding to 677 OTUs). Diagnostic rarefaction curves are shown in Supporting Information Fig. S12.

We note that a lower 16S rDNA similarity threshold (97%) was historically used for clustering bacterial and archaeal OTUs (Gevers *et al.*, 2005). Recent work, however, showed that a higher similarity threshold (99%−100%) is needed to distinguish ecologically differentiated clades (Martiny *et al.*, 2009; Koeppel and Wu, 2014), and that taxa defined based on a 97% similarity threshold may be underspeciated. Further, here our main goal was to maximize the accuracy of subsequent functional annotations of OTUs (Fig. 2B), and increasing the similarity threshold reduced the risk of lumping together functionally different species or strains during OTU clustering.

Taxonomic identification of OTUs was performed using uclust (Edgar, 2010) and the SILVA 16S reference database (release 119, Pruesse *et al.*, 2007), using the first 50 hits at a similarity threshold of at least 90% as follows: for any queried representative sequence, if at least one hit had a similarity $s \geq 99\%$, then all hits with similarity s were used to form a consensus taxonomy. Otherwise, if at least one hit had a similarity $s \geq 90\%$, then all hits with similarity at least $(s-1\%)$ were used to form a consensus taxonomy. If a query did not match any reference sequence at or above 90% similarity, it was considered unassigned and was omitted from subsequent analyses. 2047 bacterial and archaeal OTUs ($\sim$97% of total), representing 2 673 601 sequences ($\sim$98% of total), could be identified at some taxonomic level (e.g. species, genus or higher).

Metagenomic sequencing

Extracted DNA was sequenced in 100-bp paired-end fragments on an Illumina HiSeq 2000™. Library preparation and

sequencing was done by the Biodiversity Research Centre NextGen Sequencing Facility and followed standard Illumina protocols (2011 Illumina™, all rights reserved). All uniquely barcoded samples were sequenced together on a single lane. The resulting sequence data were processed using Illumina's CASAVA-1.8.2. Specifically, output files were converted to fastq format, and sequences were separated by barcode (allowing one mismatched base pair), using the configureBclToFastq.pl script. This yielded a total of 116 048 258 quality-filtered paired-end reads. Reads were trimmed at the beginning and end to increase average read quality, yielding an average forward and reverse read length of 97 and 98 bp respectively. Sufficiently overlapping paired-end reads were merged using PEAR 0.9.8 with default options (Zhang *et al*., 2014), yielding 14 702 941 merged reads. Non-merged read pairs were deduplicated using the SOFA pipeline (Hahn *et al*., 2015) and the KEGG protein reference database (Kanehisa and Goto, 2000), in order to reduce potential double-counts during subsequent gene annotation. MetaPathways 2.5 (Konwar *et al*., 2015) was used for ORF prediction in all merged and non-merged reads (min length 30, algorithm prodigal), yielding 160 979 997 ORFs. ORFs were taxonomically identified in MetaPathways using LAST and the NCBI RefSeq protein database (release 2015.12.12) (Tatusova *et al*., 2014), and ambiguous taxonomic annotations were consolidated using a lowest common ancestor algorithm (Konwar *et al*., 2015). ORFs not identified as bacterial or archaeal were omitted from further analysis. LAST annotation of ORFs against the KEGG protein reference database was performed using MetaPathways (KEGG release 2011.06.18, min BSR 0.4, max E-value 10^{-6}, min score 20, min peptide length 30, top hit), yielding 39 971 034 annotations. Metagenomic KEGG orthologous group (KOG) counts (Kanehisa and Goto, 2000) were normalized using the total number of KEGG-annotated bacterial and archaeal sequences per sample (total sum scaling).

Metagenomic KOGs were grouped into broader functional groups (e.g. oxygenic photoautotrophy or methanogenesis) based on the KEGG metabolic network database (Kanehisa and Goto, 2000). We note that some of the functional groups overlap in terms of genes associated with them; for example, all genes included in 'oxygenic photoautotrophy' were also included in 'photoautotrophy'. Because some genes (e.g. *pufM*) may have been involved in either anoxygenic photoautotrophy and/or photoheterotrophy, we did not include those genes as proxies for photoautotrophy. An overview of KOGs associated with each function is provided in Table S4.

Comparing bromeliads to lake sediments and soil

To compare the microbial communities in bromeliads with various freshwater lake sediments and soil, we considered an urban freshwater lake in Vancouver, Canada ('Trout Lake'), a freshwater lake on the East Brazilian coastline ('Lake Jacarepia', one sample), three freshwater lakes in Massachusetts, USA (two samples from 'Uncas Pond', two samples from 'Doe Pond' and one sample from 'Pickerel Pond'), three lakes on the Tibetan Plateau ('Lake Ranwu Co', 'Lake Lang Co' and 'Lake Sumxi Co', one sample each, salinities <2 g/L; Xiong *et al*., 2012), four agricultural soils (two samples from Ontario, Canada, two samples from California, USA and three samples from Western Kenya), one taiga soil from Alaska, USA (two samples) and soil from the Jurubatiba National Park, Brazil (two samples). In all cases, samples were taken from surface sediments (upper 22 cm) and surface soil (upper 20 cm).

Near-shore sediments (upper 10 cm of sediments, water depth $\sim$1 m) were collected from Trout Lake, Vancouver, by our group in July 2014 (two replicate samples) and in August 2014 (two replicate samples). Samples were placed on ice in the field for 1 h and frozen in the lab at -80°C until further processing. DNA was extracted, 16S rRNA genes were amplified, amplicons were sequenced and sequences were processed exactly as with the bromeliad samples, yielding 739 OTUs accounting for a total of 21 661 reads. Reads from replicate samples were subsequently combined in the OTU table. Soil samples from Jurubatiba National Park were collected from the soil surface (upper 10 cm) at two locations, on the same day as the bromeliads. One soil type was a dry mixture of sand and brown detritus in a canopy-covered location, the other type was red, extremely dry and completely exposed. Soil samples from Jurubatiba were treated in the exact same manner as the bromeliad detritus. After sequencing and processing, a total of 513 OTUs were obtained, accounting for 163 219 reads across two samples.

For the remaining nine lake sediment samples and the remaining nine soil samples, pre-processed sequence data were obtained from the Earth Microbiome Project (EMP) database (http://www.earthmicrobiome.org; Gilbert *et al*., 2014), in the form of an OTU table with representative sequences (OTUs closed-reference picked using SILVA 123 at 97% similarity; sample overview in Table S2). For consistency with our other analyses, we re-classified OTUs from the EMP data set taxonomically using the SILVA reference database (release 119, Pruesse *et al*., 2007) with vsearch (Rognes *et al*., 2016), at an acceptance threshold of 99% similarity. Out of the 25 736 bacterial and archaeal OTUs in the original EMP data set, a total of 23 497 OTUs could be mapped this way to SILVA, accounting for 1 862 383 reads across 18 samples.

Functional annotation of bacterial and archaeal taxa

To facilitate the interpretation of metagenomic functional profiles, we also associated detected organisms with one or more metabolic functions based on available literature on cultured representatives, whenever possible. Details of this approach, which we outline here, are provided by Louca *et al*. (2016b). In short, a taxon (e.g. strain, species or genus) was associated with a particular metabolic function if all cultured representatives within the taxon have been reported to exhibit that function. For example, if a detected organism was identified within a bacterial genus whose cultured member species have all been found to be methanotrophs, we considered that organism to also be a methanotroph. We stress that as more organisms are cultured in the future, some of these generalizations may turn out to be erroneous. Our complete database for the functional annotation of bacterial and archaeal (prokaryotic) taxa (FAPROTAX) includes over 7600 annotations and covers over 4600 taxa, and is available at: www.zoology.ubc.ca/louca/FAPROTAX. A detailed evaluation of FAPROTAX, including a direct comparison with metagenomics, is provided by Louca *et al*. (2016b).

Across all bromeliads, a total of 520 OTUs (25.4% of those taxonomically identified) were assigned to at least one of the 15 considered functional groups, yielding a total of 604 functional annotations (overview in Fig. 2B and Supporting Information Table S5). The complete list of functional annotations, including supporting literature, is available as Supporting Information Data 1. Throughout the paper, unless otherwise mentioned, OTU-based relative abundances of functional groups are given with respect to the total number of sequences that could be assigned to at least one functional group. For example, a relative abundance of 16% methanogens means that 16% of the sequences assigned to some functional group were assigned to the group of putative methanogens.

Functional annotation of OTUs found in lake sediments and soil was performed as described above for bromeliads. A total of 192 OTUs from the Trout Lake samples could be assigned to at least one functional group, yielding a total of 200 functional annotations. OTUs from Jurubatiba soil samples and bromeliads were functionally annotated at the same time; 535 out of 2201 OTUs could be assigned to at least one functional group, yielding 628 functional annotations. From the EMP samples, 6197 out of 23 497 OTUs could be assigned to at least one functional group, yielding a total of 7037 functional annotations.

Statistical analyses

Correlation analysis. To assess the extent to which environmental conditions related to functional community structure, we calculated Spearman rank correlations between the relative abundances of individual metagenomic functional groups on the one hand, and various environmental variables on the other hand. Environmental variables were absorption at 440 nm wavelength ('water color'), dissolved organic carbon (DOC), light intensity at noon, methane concentration, total molar N:P ratio, the number of plant leaves, pH, plant height, salinity, canopy coverage, detrital volume, total tank depth (bottom to water surface), total (organic + inorganic) P, total (organic + inorganic) N, total suspended solids (TSS), total tank volume (detritus + overlying water) and turbidity (overview in Fig. 1). Oxygen concentration, temperature and nitrous oxide concentration were not considered in the correlation analysis, because oxygen and temperature varied strongly throughout the day and were not measured concurrently, and because most nitrous oxide concentrations were below the detection limit. The statistical significance of correlations between metagenomic functional groups and environmental variables was estimated through 10^4 random permutations. In the main text we present correlations across all 31 bromeliads (Fig. 3), however some of these correlations may be driven by systematic differences between bromeliad species. We thus also provide correlations restricted to a single bromeliad species, *A. nudicaulis*, as Supporting Information (Fig. S9).

Comparing microbial communities between habitats. To test whether microbial communities differed systematically between bromeliad species, we performed PERMANOVA resemblance analysis (Anderson, 2001) of pairwise community dissimilarities (Legendre and Legendre, 1998). The statistical significance of the resulting pseudo-F statistic was estimated using 10^4 random permutations. Dissimilarities were calculated using the Bray-Curtis metric (Legendre and Legendre, 1998), in terms of the relative abundances of taxa (at various taxonomic levels), metagenomic functional groups (as listed in Fig. 2A), KEGG orthologous groups (KOG) and standard KEGG categories (levels B and C; overview in Table S1). Prior to calculating dissimilarities, we rarefied (i.e. subsampled without replacement) all samples to the maximum possible equal sequencing depth (5565 16S rRNA sequences for taxa, 22 472 metagenomic sequences for KOGs and 929 metagenomic sequences for functional groups). Rarefaction was repeated 1000 times to obtain an averaged dissimilarity matrix.

To test whether specific taxa (or metagenomic functional groups, KOGs or KEGG categories) were overrepresented in one bromeliad species compared to the other (in terms of their relative abundances), we performed permutation tests using the Welch test statistic (Welch, 1947). The Welch statistic for a particular taxon is defined as

$$T = \frac{\bar{X}_1 - \bar{X}_2}{\sqrt{\frac{\sigma_1^2}{N_1} + \frac{\sigma_2^2}{N_2}}}, \quad (1)$$

where $\bar{X}_i$ and σ_i^2 are the sample mean and sample variance, respectively, of the relative taxon abundances in the ith bromeliad species ($i = 1, 2$), and N_i is the number of bromeliads of species i. A positive T corresponds to an overrepresentation of the taxon in bromeliad species 1, but the magnitude of T is smaller when the variance σ_i^2 within each species is larger. The statistical significance of T under the null hypothesis of equal distributions in each species, that is the probability that a random T would have greater magnitude than observed, was estimated through 10^4 repeated permutations of the samples. Note that, in contrast to the original Welch test (Welch, 1947), this permutation null model does not assume normal distributions for relative taxon abundances. When counting the number of taxa with significant T, we did not account for multiple tests (e.g. using a Bonferroni correction), because such a correction would be overly conservative for our low sample sizes. Instead, to assess the overall extent to which taxa are differentially represented between bromeliad species, the fraction of taxa exhibiting a significant T should be compared to the type I error rate expected under the null hypothesis (5%). A similar approach to the above was taken for metagenomic functional groups, KOGs and KEGG categories. An overview of the permutations tests is provided in Table S1.

PERMANOVA analysis of pairwise taxonomic Bray-Curtis dissimilarities was also performed between bromeliads and lake sediments as well as between bromeliads and soil, as described above for the comparison between bromeliad species. To visualize pairwise dissimilarities, we used metric multidimensional scaling (MDS; Borg and Groenen, 2005). In MDS, sample points are embedded into a reduced number of dimensions (e.g. 2) such that the pairwise Euclidean sample distances in the embedding 'best match' the original dissimilarities. Hence, points that are closer to each other in the embedding correspond to samples with more similar microbial communities. The embedding was performed by minimizing

the Kruskal stress, using the Scikit-lean package (Pedregosa *et al*., 2011). To test whether specific taxa were mostly found in bromeliads, in lake sediments or in soil, we used a similar (but not identical) permutation approach as above, with the following modification: We first converted OTU tables to presence-absence format, and then considered the simplified test statistic $T = \bar{X}_i - \bar{X}_j$ for each taxon, where $\bar{X}_i$ is the fraction of samples of some type *i* (bromeliads, lake sediment or soil) in which the taxon was detected. Hence, a statistically significant *T* for a particular taxon and a particular pair of environments (bromeliads vs. lake sediments or bromeliads vs. soil) means that the taxon was more frequently detected in one of the two environments. A presence-absence-based test was chosen instead of a relative-abundance-based test because microbial communities differed drastically between the considered environments, and thus the relative abundance of any given taxon was strongly influenced by the abundances of other taxa in each location. For each pair of compared environments we only considered taxa found in at least one of the two environments (e.g. when comparing bromeliads to soil we ignored taxa only found in lake sediments). For all statistical comparisons between bromeliad, lake sediment and soil microbial communities, we rarefied OTU tables to the maximum possible equal sequencing depth (4930 16S rRNA sequences per sample). An overview of the permutation tests is provided in Table S3.

Sequence data availability. Molecular sequence data generated by this project have been deposited in the NCBI BioProject database (BioProject no. PRJNA321235; www.ncbi.nlm.nih.gov/bioproject), with sample accession nos. SRS1433623–SRS1433644, SRS1972256–SRS1972264 and SRS1997243–SRS1997244; run accession nos. SRR3498561–SRR3498582, SRR5248624–SRR5248632 and SRR5279582–SRR5279583 (16S amplicons), and SRR3498952–SRR3498973 and SRR5248713–SRR5248721 (metagenomes). Accession numbers for data obtained from the Earth Microbiome Project are listed in Supporting Information Table S2.

Acknowledgements

We thank Laura W. Parfrey for providing her laboratory for molecular work. We thank Melissa Chen for advice on the molecular work. We thank Diane Srivastava for discussions and comments on our paper. S. L. and M. D. acknowledge the support of NSERC. V. F. F. is grateful to the Brazilian Council for Research, Development and Innovation (CNPq) for research funds (PVE Research Grant 400454/2014–9) and productivity grants. S. M. S. J. acknowledges the postgraduate scholarship provided by Filho de Amparo a Pesquisa do Estado do Rio de Janeiro (FAPERJ). J. S. L. acknowledges the financial support of Coordenação de Aperfeiçoamento de Pessoal de Ensino Superior (CAPES). We thank Marcos Paulo F. Barros, Angelica R. Soares, Jose L. Nepomuceno, and their research groups of the Nucleus of Ecology and Socio-Environmental Development of Macaé (NUPEM/UFRJ) for proving field and laboratory assistance during the samplings.

Author contributions

S. L., V. F. F., S. M. S. J., A. P. F. P., and J. S. L. performed the field work. V. F. F. and S. M. S. J. performed the chemical measurements in the laboratory. S. L. performed the molecular work in the laboratory, the DNA sequence analysis and the statistical analyses. All authors contributed to the writing of the manuscript. V. F. F., A. L. G., and M. D. supervised the project.

References

Anderson, M.J. (2001) A new method for non-parametric multivariate analysis of variance. *Austral Ecol* **26:** 32–46.

Anderson, M.J., and Walsh, D.C. (2013) PERMANOVA, ANOSIM, and the Mantel test in the face of heterogeneous dispersions: What null hypothesis are you testing? *Ecol Monograph* **83:** 557–574.

Atwood, T.B., Hammill, E., Greig, H.S., Kratina, P., Shurin, J.B., Srivastava, D.S., *et al*. (2013) Predator-induced reduction of freshwater carbon dioxide emissions. *Nat Geosci* **6:** 191–194.

Benzing, D.H., and Renfrow, A. (1974) The mineral nutrition of Bromeliaceae. *Botanical Gazette* **135:** 281–288.

Borg, I., and Groenen, P.J.F. (2005) *Modern Multidimensional Scaling: Theory and Applications. Springer Series in Statistics*, 2nd ed. New York: Springer.

Bouard, O., Céréghino, R., Corbara, B., Leroy, C., Pelozuelo, L., Dejean, A., *et al*. (2012) Understorey environments influence functional diversity in tank-bromeliad ecosystems. *Freshwater Biol* **57:** 815–823.

Brandt, F.B., Martinson, G.O., and Conrad, R. (2016) Bromeliad tanks are unique habitats for microbial communities involved in methane turnover. *Plant Soil* **410:** 167–179.

Brandt, F.B., Martinson, G.O., Pommerenke, B., Pump, J., and Conrad, R. (2015) Drying effects on archaeal community composition and methanogenesis in bromeliad tanks. *FEMS Microbiol Ecol* **91:** 1–10.

Brighigna, L., Montaini, P., Favilli, F., and Trejo, A.C. (1992) Role of the nitrogen-fixing bacterial microflora in the epiphytism of Tillandsia (Bromeliaceae). *Am J Botany* **79:** 723–727.

Bryant, D.A., and Frigaard, N.U. (2006) Prokaryotic photosynthesis and phototrophy illuminated. *Trend Microbiol* **14:** 488–496.

Canfield, D.E., Glazer, A.N., and Falkowski, P.G. (2010) The evolution and future of Earth's nitrogen cycle. *Science* **330:** 192–196.

Canfield, D.E., and Thamdrup, B. (2009) Towards a consistent classification scheme for geochemical environments, or, why we wish the term 'suboxic' would go away. *Geobiology* **7:** 385–392.

Capone, D.G., and Kiene, R.P. (1988) Comparison of microbial dynamics in marine and freshwater sediments: Contrasts in anaerobic carbon catabolism. *Limnol Oceanograph* **33:** 725–749.

Caporaso, J.G., Kuczynski, J., Stombaugh, J., Bittinger, K., Bushman, F.D., Costello, E.K., *et al*. (2010) QIIME allows analysis of high-throughput community sequencing data. *Nat Method* **7:** 335–336.

Caporaso, J.G., Lauber, C.L., Walters, W.A., Berg-Lyons, D., Huntley, J., Fierer, N., *et al*. (2012) Ultra-high-throughput microbial community analysis on the Illumina HiSeq and MiSeq platforms. *ISME J* **6:** 1621–1624.

Chung, E.J., Park, T.S., Jeon, C.O., and Chung, Y.R. (2012) *Chitinophaga oryziterrae* sp. nov., isolated from the rhizosphere soil of rice (*Oryza sativa* l.). *Int J Syst Evol Microbiol* **62:** 3030–3035.

Cogliatti-Carvalho, L., Freitas, A.D., Rocha, C.D., and Van Sluys, M. (2001) Variação na estrutura e na composição de Bromeliaceae em cinco zonas de restinga no Parque Nacional da Restinga de Jurubatiba, Macaé, RJ. *Revista Brasileira De Botânica* **24:** 1–9.

Dalsgaard, T., Thamdrup, B., and Canfield, D.E. (2005) Anaerobic ammonium oxidation (anammox) in the marine environment. *Res Microbiol* **156:** 457–464.

Dworkin, M., Falkow, S., Rosenberg, E., Schleifer, K., and Stackebrandt, E. (2014) *The Prokaryotes*. New York: Springer.

Edgar, R.C. (2010) Search and clustering orders of magnitude faster than BLAST. *Bioinformatics* **26:** 2460–2461.

Elser, J., Chrzanowski, T., Sterner, R., Schampel, J., and Foster, D. (1995) Elemental ratios and the uptake and release of nutrients by phytoplankton and bacteria in three lakes of the Canadian shield. *Microbial Ecol* **29:** 145–162.

Endres, L., and Mercier, H. (2003) Amino acid uptake and profile in bromeliads with different habits cultivated in vitro. *Plant Physiol Biochem* **41:** 181–187.

Evans, P.N., Parks, D.H., Chadwick, G.L., Robbins, S.J., Orphan, V.J., Golding, S.D., *et al*. (2015) Methane metabolism in the archaeal phylum Bathyarchaeota revealed by genome-centric metagenomics. *Science* **350:** 434–438.

Farjalla, V.F., González, A.L., Céréghino, R., Dézerald, O., Marino, N.A.C., Piccoli, G.C.O., *et al*. (2016) Terrestrial support of aquatic food webs depends on light inputs: a geographically-replicated test using tank bromeliads. *Ecology* **97:** 2147–2156.

Farjalla, V.F., Srivastava, D.S., Marino, N.A.C., Azevedo, F.D., Dib, V., Lopes, P.M., *et al*. (2012) Ecological determinism increases with organism size. *Ecology* **93:** 1752–1759.

Fillol, M., Sànchez-Melsió, A., Gich, F., and M. Borrego, C. (2015) Diversity of miscellaneous crenarchaeotic group archaea in freshwater karstic lakes and their segregation between planktonic and sediment habitats. *FEMS Microbiol Ecol* **91:** fiv020.

Fofonoff, N.P., and Millard-Junior, R. (1983) Algorithms for computation of fundamental properties of seawater. Technical report, UNESCO technical papers in marine science.

Garrity, G. (2001) *Bergey's Manual of Systematic Bacteriology, Bergey's Manual of Systematic Bacteriology*, Vol. 1. New York: Springer.

Garrity, G. (2005) *Bergey's Manual of Systematic Bacteriology: Volume 2: The Proteobacteria, Bergey's Manual of Systematic Bacteriology*. New York: Springer.

Gevers, D., Cohan, F.M., Lawrence, J.G., Spratt, B.G., Coenye, T., Feil, E.J., *et al*. (2005) Re-evaluating prokaryotic species. *Nat Rev Microbiol* **3:** 733–739.

Gilbert, J.A., Jansson, J.K., and Knight, R. (2014) The Earth Microbiome project: successes and aspirations. *BMC Biol* **12:** 69.

Giongo, A., Beneduzi, A., Gano, K., Vargas, L.K., Utz, L., and Passaglia, L.M.P. (2013) Characterization of plant growth-promoting bacteria inhabiting Vriesea gigantea Gaud. and Tillandsia aeranthos (Loiseleur) L.B. Smith (Bromeliaceae). *Biota Neotropica* **13:** 80–85.

Goffredi, S.K., Jang, G., Woodside, W.T., and Ussler, W. (2011a) Bromeliad catchments as habitats for methanogenesis in tropical rainforest canopies. *Front Microbiol* **2:** 256.

Goffredi, S.K., Jang, G.E., and Haroon, M.F. (2015) Transcriptomics in the tropics: Total RNA-based profiling of Costa Rican bromeliad-associated communities. *Comput Struct Biotechnol J* **13:** 18–23.

Goffredi, S.K., Kantor, A.H., and Woodside, W.T. (2011b) Aquatic microbial habitats within a neotropical rainforest: Bromeliads and pH-associated trends in bacterial diversity and composition. *Microbial Ecol* **61:** 529–542.

Golterman, H., Clymo, R., and Ohnstad, M. (1978) Methods for physical and chemical analysis of fresh waters. *Int Rev Hydrobiol* **65:** 169.

González, A.L., Romero, G.Q., and Srivastava, D.S. (2014) Detrital nutrient content determines growth rate and elemental composition of bromeliad-dwelling insects. *Freshwater Biol* **59:** 737–747.

Guimaraes-Souza, B., Mendes, G., Bento, L., Marotta, H., Santoro, A., Esteves, F., *et al*. (2006) Limnological parameters in the water accumulated in tropical bromeliads. *Acta Limnologica Brasiliensia* **18:** 47–53.

Hahn, A., Hanson, N., Kim, D., Konwar, K., and Hallam, S. (2015) Assembly independent functional annotation of short-read data using SOFA: Short-ORF functional annotation. In *Computational Intelligence in Bioinformatics and Computational Biology (CIBCB), 2015 IEEE Conference on, pp. 1–6*. IEEE.

Haubrich, C.S., Pires, A.P.F., Esteves, F.A., and Farjalla, V.F. (2009) Bottom-up regulation of bacterial growth in tropical phytotelm bromeliads. *Hydrobiologia* **632:** 347–353.

Hinrichs, K.U., and Boetius, A. (2003) *The Anaerobic Oxidation of Methane: New Insights in Microbial Ecology and Biogeochemistry*. Berlin: Springer, pp. 457–477.

Hinsley, A.P., and Berks, B.C. (2002) Specificity of respiratory pathways involved in the reduction of sulfur compounds by *Salmonella enterica*. *Microbiology* **148:** 3631–3638.

Iversen, N., and Jørgensen, B.B. (1993) Diffusion coefficients of sulfate and methane in marine sediments: Influence of porosity. *Geochimica Et Cosmochimica Acta* **57:** 571–578.

Kanehisa, M., and Goto, S. (2000) KEGG: Kyoto Encyclopedia of genes and genomes. *Nucl Acid Res* **28:** 27–30.

Kisand, V., and Wikner, J. (2003) Limited resolution of 16S rDNA DGGE caused by melting properties and closely related DNA sequences. *J Microbiol Method* **54:** 183–191.

Kitching, R. (2000) *Food Webs and Container Habitats: The Natural History and Ecology of Phytotelmata*. Cambridge: Cambridge University Press.

Kitching, R. (2001) Food webs in phytotelmata: 'Bottom-up' and 'top-down' explanations for community structure. *Ann Rev Entomol* **46:** 729–760.

Kodama, Y., and Watanabe, K. (2011) *Rhizomicrobium electricum* sp. nov., a facultatively anaerobic, fermentative,

prosthecate bacterium isolated from a cellulose-fed microbial fuel cell. *Int J Syst Evol Microbiol* **61:** 1781–1785.
Koeppel, A.F., and Wu, M. (2014) Species matter: The role of competition in the assembly of congeneric bacteria. *ISME J* **8:** 531–540.
Konwar, K.M., Hanson, N.W., Bhatia, M.P., Kim, D., Wu, S.J., Hahn, A.S., *et al*. (2015) MetaPathways v2.5: Quantitative functional, taxonomic and usability improvements. *Bioinformatics* **31:** 3345–3347.
Legendre, P., and Legendre, L. (1998) *Numerical Ecology. Developments in Environmental Modelling*, 2nd ed. Amsterdam: Elsevier Science B.V.
Lehours, A.C., Jeune, A.H.L., Aguer, J.P., Céréghino, R., Corbara, B., Kéraval, B., *et al*. (2016) Unexpectedly high bacteriochlorophyll a concentrations in neotropical tank bromeliads. In *Environmental Microbiology Reports*.
Li, W., Fu, L., Niu, B., Wu, S., and Wooley, J. (2012) Ultrafast clustering algorithms for metagenomic sequence analysis. *Brief Bioinform* **13:** 656–668.
Lloyd, K.G., Schreiber, L., Petersen, D.G., Kjeldsen, K.U., Lever, M.A., Steen, A.D., *et al*. (2013) Predominant archaea in marine sediments degrade detrital proteins. *Nature* **496:** 215–218.
Louca, S., Jacques, S.M.S., Pires, A.P.F., Leal, J.S., Srivastava, D.S., Parfrey, L.W., *et al*. (2016a) High taxonomic variability despite stable functional structure across microbial communities. *Nat Ecol Evol* **1:** 0015.
Louca, S., Parfrey, L.W., and Doebeli, M. (2016b) Decoupling function and taxonomy in the global ocean microbiome. *Science* **353:** 1272–1277.
Madigan, M.T., and Jung, D.O. (2009) *The Purple Phototrophic Bacteria, Chapter an Overview of Purple Bacteria: Systematics, Physiology, and Habitats*. Dordrecht: Springer, pp. 1–15.
Marino, N.A.C., Srivastava, D.S., and Farjalla, V.F. (2013) Aquatic macroinvertebrate community composition in tank-bromeliads is determined by bromeliad species and its constrained characteristics. *Insect Conservat Diversity* **6:** 372–380.
Martinson, G.O., Werner, F.A., Scherber, C., Conrad, R., Corre, M.D., Flessa, H., *et al*. (2010) Methane emissions from tank bromeliads in neotropical forests. *Nat Geosci* **3:** 766–769.
Martiny, A.C., Tai, A.P., Veneziano, D., Primeau, F., and Chisholm, S.W. (2009) Taxonomic resolution, ecotypes and the biogeography of *Prochlorococcus*. *Environ Microbiol* **11:** 823–832.
Moran, M.A., Satinsky, B., Gifford, S.M., Luo, H., Rivers, A., Chan, L.K., *et al*. (2013) Sizing up metatranscriptomics. *ISME J* **7:** 237–243.
Ngai, J.T., and Srivastava, D.S. (2006) Predators accelerate nutrient cycling in a bromeliad ecosystem. *Science* **314:** 963–963.
Parte, A., Krieg, N., Ludwig, W., Whitman, W., Hedlund, B., Paster, B., *et al*. (2011) *Bergey's Manual of Systematic Bacteriology: Volume 4: The Bacteroidetes, Spirochaetes, Tenericutes (Mollicutes), Acidobacteria, Fibrobacteres, Fusobacteria, Dictyoglomi, Gemmatimonadetes, Lentisphaerae, Verrucomicrobia, Chlamydiae, and Planctomycetes. Bergey's Manual of Systematic Bacteriology*. New York: Springer.
Pedregosa, F., Varoquaux, G., Gramfort, A., Michel, V., Thirion, B., Grisel, O., *et al*. (2011) Scikit-learn: Machine learning in Python. *J Machine Learn Res* **12:** 2825–2830.
Pittendrigh, C.S. (1948) The bromeliad-anopheles-malaria complex in Trinidad. I-The bromeliad flora. *Evolution* **2:** 58–89.
Pruesse, E., Quast, C., Knittel, K., Fuchs, B.M., Ludwig, W., Peplies, J., *et al*. (2007) SILVA: A comprehensive online resource for quality checked and aligned ribosomal RNA sequence data compatible with ARB: A comprehensive online resource for quality checked and aligned ribosomal RNA sequence data compatible with ARB. *Nucl Acid Res* **35:** 7188–7196.
Ramana, V.V., Raj, P.S., Tushar, L., Sasikala, C., and Ramana, C.V. (2013) *Rhodomicrobium udaipurense* sp. nov., a psychrotolerant, phototrophic alphaproteobacterium isolated from a freshwater stream. *Int J Syst Evol Microbiol* **63:** 2684–2689.
Richardson, B.A. (1999) The bromeliad microcosm and the assessment of faunal diversity in a neotropical forest. *Biotropica* **31:** 321–336.
Rocha, C., Cogliatti-Carvalho, L., Almeida, D., and Freitas, A. (2000) Bromeliads: Biodiversity amplifiers. *J Bromeliad Soc* **50:** 81–83.
Rognes, T., Flouri, T., Nichols, B., Quince, C., and Mahé, F. (2016) VSEARCH: A versatile open source tool for metagenomics. *PeerJ* **4:** e2584.
Romero, G.Q., Mazzafera, P., Vasconcellos-Neto, J., and Trivelin, P.C.O. (2006) Bromeliad-living spiders improve host plant nutrition and growth. *Ecology* **87:** 803–808.
Sardans, J., Rivas-Ubach, A., and Peñuelas, J. (2011) The elemental stoichiometry of aquatic and terrestrial ecosystems and its relationships with organismic lifestyle and ecosystem structure and function: a review and perspectives. *Biogeochemistry* **111:** 1–39.
Serrano-Silva, N., Sarria-Guzmán, Y., Dendooven, L., and Luna-Guido, M. (2014) Methanogenesis and methanotrophy in soil: A review. *Pedosphere* **24:** 291–307.
Srivastava, D.S. (2006) Habitat structure, trophic structure and ecosystem function: interactive effects in a bromeliad–insect community. *Oecologia* **149:** 493–504.
Srivastava, D.S., Kolasa, J., Bengtsson, J., Gonzalez, A., Lawler, S.P., Miller, T.E., *et al*. (2004) Are natural microcosms useful model systems for ecology?. *Trend Ecol Evol* **19:** 379–384.
Tatusova, T., Ciufo, S., Fedorov, B., O'Neill, K., and Tolstoy, I. (2014) RefSeq microbial genomes database: New representation and annotation strategy. *Nucl Acid Res* **42:** D553–D559.
Vos, P., Garrity, G., Jones, D., Krieg, N., Ludwig, W., Rainey, F., *et al*. (2011) *Bergey's Manual of Systematic Bacteriology: Volume 3: The Firmicutes. Bergey's Manual of Systematic Bacteriology*. New York: Springer.
Welch, B.L. (1947) The generalization of 'student's' problem when several different population variances are involved. *Biometrika* **34:** 28–35.
Wetzel, R. (2001) *Limnology: Lake and River Ecosystems*, 3rd edn. San Diego: Academic Press.
Xiong, J., Liu, Y., Lin, X., Zhang, H., Zeng, J., Hou, J., *et al*. (2012) Geographic distance and pH drive bacterial distribution in alkaline lake sediments across tibetan plateau. *Environ Microbiol* **14:** 2457–2466.

Zagatto, E., Jacintho, A., Mortatti, J., and Bergamin, F.H. (1980) An improved flow injection determination of nitrite in waters by using intermittent flows. *Analytica Chimica Acta* **120:** 399–403.

Zhang, J., Kobert, K., Flouri, T., and Stamatakis, A. (2014) PEAR: A fast and accurate Illumina Paired-End reAd mergeR. *Bioinformatics* **30:** 614–620.

Zotz, G., and Asshoff, R. (2010) Growth in epiphytic bromeliads: Response to the relative supply of phosphorus and nitrogen. *Plant Biol* **12:** 108–113.

Supporting information

Additional Supporting Information may be found in the online version of this article at the publisher's web-site:

Fig. S1. Core microbiomes of bromeliads. Core microbiome size (number of shared OTUs) for any given number of randomly chosen bromeliads. The core microbiome across all 31 bromeliads comprises only 35 OTUs (horizontal reference line).

Fig. S2. Functional redundancy in the regional OTU pool, based on bromeliad samples. Association of OTUs (rows) detected in the bromeliads with various metabolic functions (columns), indicated by blue cells. Only OTUs associated with at least one function are shown. Functions are sorted according to the number of associated OTUs.

Fig. S3. Taxonomic community composition in bromeliads (family level). Relative abundances of various prokaryotic families (one column per sample, one row per family). Circle sizes are proportional to relative abundances. Only the most abundant families (i.e. comprising at least 2% in at least one sample) are shown. Families with statistically significant ($P < 0.05$) overrepresentation in *A. nudicaulis* or *N. cruenta* are indicated in red and blue respectively. For profiles at the phylum, class or order level, see Figs. S4, S10 and S11 respectively.

Fig. S4. Taxonomic community composition in bromeliads (class level). Relative abundances of various prokaryotic classes (one columns per sample, one row per class). Circle surface is proportional to relative abundance. Only classes comprising at least 2% in at least one bromeliad are shown. Samples are colored according to bromeliad species (red for *A. nudicaulis* and blue for *N. cruenta*). Classes with statistically significant ($P < 0.05$ based on permutation tests) overrepresentation in *A. nudicaulis* or *N. cruenta* are indicated in red and blue respectively. For profiles at the phylum, order and family level see Figs. S3, S10 and S11 respectively.

Fig. S5. Functional community profiles in bromeliads. (A) Metagenomic functional profiles, in terms of relative gene abundances (one column per sample, one color per functional group). Most functional groups comprise several genes or several subunits of one gene. (B) Same as (A), but only showing the 15 least abundant functional groups. For the list of genes (KEGG orthologs) included in each group, see Supporting Information Table S4. (C) Relative abundances of OTUs associated with various metabolic functions, used to facilitate the interpretation of metagenomic functional profiles.

Fig. S6. Ambiguities in functional annotations of OTUs across bromeliads. Overlaps between prokaryotic functional groups in terms of shared identified OTUs (Jaccard similarity index). A darker color corresponds to a greater overlap. An overlap of 1.0 corresponds to identical groups.

Fig. S7. Correlations between environmental variables across bromeliads. Spearman rank correlations between environmental variables across all bromeliads. Blue and red correspond to statistically significant ($P < 0.05$) positive and negative correlations respectively. White indicates zero or statistically non-significant correlations. Rows and columns are hierarchically clustered by similarity.

Fig. S8. Correlations between environmental variables (within *A. nudicaulis*). Spearman rank correlations between environmental variables across *A. nudicaulis* bromeliads. Blue and red correspond to statistically significant ($P < 0.05$) positive and negative correlations respectively. White indicates zero or statistically non-significant correlations. Rows and columns are hierarchically clustered by similarity. For correlations across all bromeliads (*A. nudicaulis* and *N. cruenta*), see Fig. S7.

Fig. S9. Metagenomic functional groups vs environmental variables (within *A. nudicaulis*). Spearman rank correlations between relative metagenomic functional group abundances and environmental variables across *A. nudicaulis* bromeliads. Blue and red colors correspond to positive and negative correlations respectively. Circle size and color saturation are proportional to the magnitude of the correlation. Statistically significant correlations ($P < 0.05$) are indicated by black perimeters. Rows and columns are hierarchically clustered by similarity. For correlations across all bromeliads (*A. nudicaulis* and *N. cruenta*), see Fig. 3.

Fig. S10. Taxonomic community composition in bromeliads (phylum level). Relative abundances of various prokaryotic phyla (one column per sample, one row per phylum). Circle sizes are proportional to relative abundances. Only the most abundant phyla (i.e. comprising at least 2% in at least one sample) are shown. None of the shown phyla exhibited a significant overrepresentation in any bromeliad species. For profiles at the class, order or family level, see Figs. S3, S4 and S11 respectively.

Fig. S11. Taxonomic community composition in bromeliads (order level). Relative abundances of various prokaryotic orders (one column per sample, one row per order). Circle sizes are proportional to relative abundances. Only the most abundant orders (i.e. comprising at least 2% in at least one sample) are shown. Orders with statistically significant ($P < 0.05$) overrepresentation in *A. nudicaulis* or *N. cruenta* are indicated in red and blue respectively. For profiles at the phylum, class or family level, see Figs. S3, S4 and S10 respectively.

Fig. S12. 16S rDNA rarefaction curves for bromeliads (OTU richness). Each plot: expected number of observed distinct OTUs at various sequencing depths for a particular bromeliad, determined through repeated random rarefactions. Bromeliad IDs are provided in the figures.

Table S1. Comparisons between bromeliad species. Statistical comparison of prokaryotic community structure between bromeliad species, *A. nudicaulis* and *N. cruenta*, in terms of the taxa, gene groups (as listed in Fig. 2A), KEGG orthologous groups (KOG) and KEGG categories (level B & C). Also listed are the fractions of taxa, gene groups, KOGs or KEGG categories whose mean relative

abundances differed significantly ($P < 0.05$) between the two bromeliad species.

Table S2. Overview of third party samples. Overview of freshwater sediment and soil 16S sequencing samples obtained from the Earth Microbiome Project (EMP, http://www.earthmicrobiome.org), for comparison with the bromeliads. The table includes the original EMP sample IDs, as well as run accessions at the European Nucleotide Archive (http://www.ebi.ac.uk/ena) and the original publication (if available). Metadata were obtained from the accessions, the original publication or from the EMP database (ftp.microbio.me/emp).

Table S3. Comparing taxon occurrences in bromeliads to lake sediments and soil. Fractions of taxa whose occurrence frequency (i.e. the number of samples in which they were detected) differed significantly ($P < 0.05$) between bromeliads and freshwater lake sediments, or between bromeliads and soil. Statistical significances were calculated using the Welch statistic and permutation tests.

Table S4. KOG-function associations. KEGG gene orthologous groups (KOG) associated with various functions in the metagenomic sequences.

Table S5. Numbers of functionally annotated OTUs in bromeliads. Number of OTUs associated with each metabolic function, compared to the total number of taxonomically annotated OTUs. Some OTUs were associated with multiple functions (Fig. S2).

Functional structure of the bromeliad tank microbiome is strongly shaped by local geochemical conditions
- Supplementary Material -

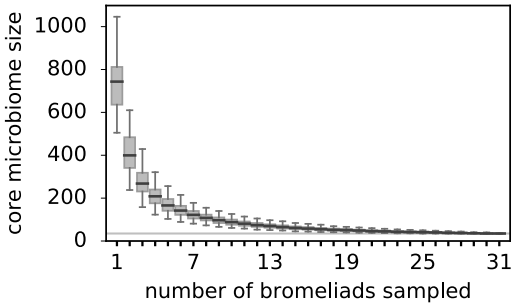

Figure S1: **Core microbiomes of bromeliads.** Core microbiome size (number of shared OTUs) for any given number of randomly chosen bromeliads. The core microbiome across all 31 bromeliads comprises only 35 OTUs (horizontal reference line).

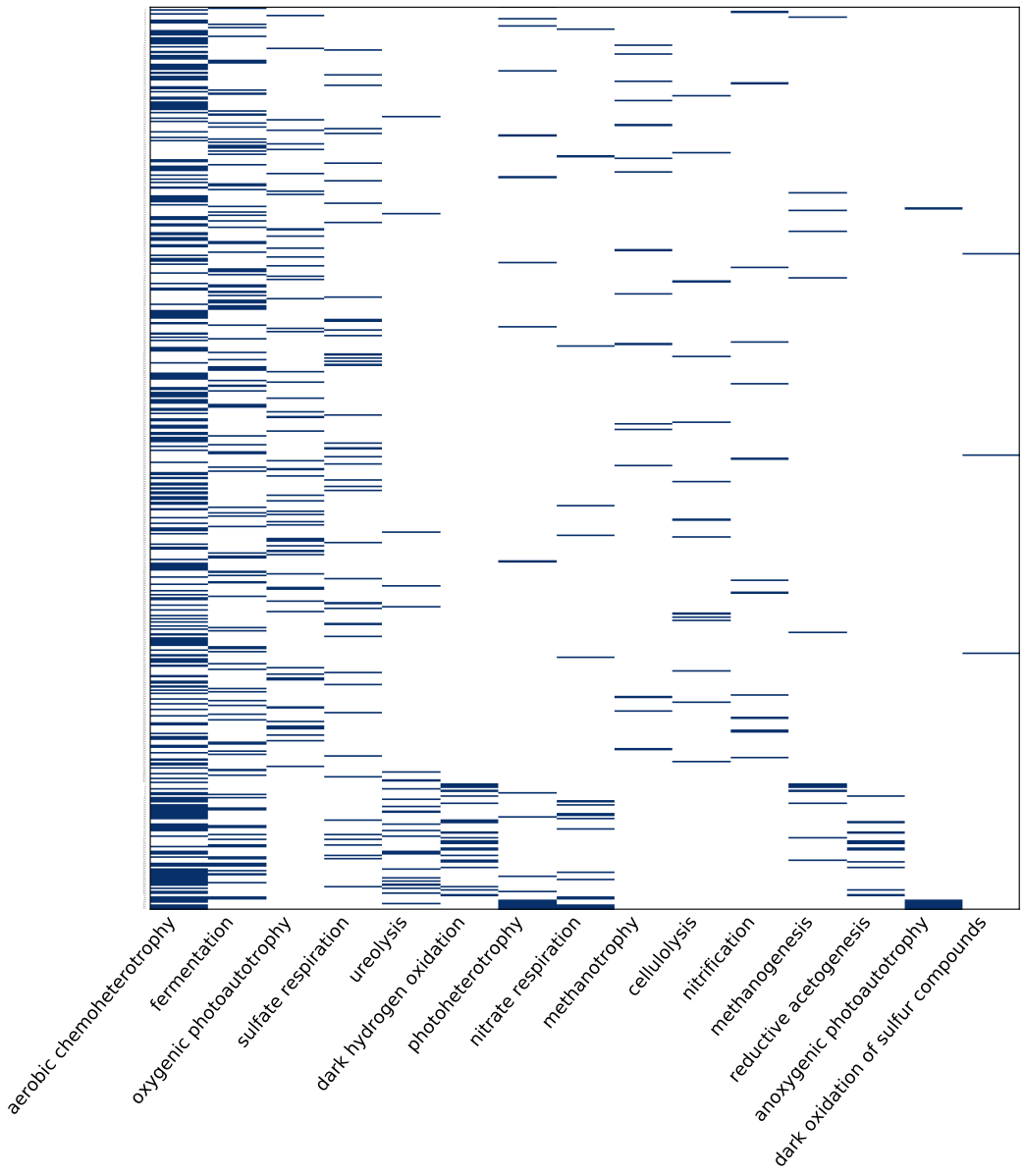

Figure S2: **Functional redundancy in the regional OTU pool, based on bromeliad samples.** Association of OTUs (rows) detected in the bromeliads with various metabolic functions (columns), indicated by blue cells. Only OTUs associated with at least one function are shown. Functions are sorted according to the number of associated OTUs.

Figure S3: **Taxonomic community composition in bromeliads (family level).** Relative abundances of various prokaryotic families (one column per sample, one row per family). Circle sizes are proportional to relative abundances. Only the most abundant families (i.e. comprising at least 2% in at least one sample) are shown. Families with statistically significant ($P < 0.05$) overrepresentation in *A. nudicaulis* or *N. cruenta* are indicated in red and blue, respectively. For profiles at the phylum, class or order level, see Figs. S10, S4 and S11, respectively.

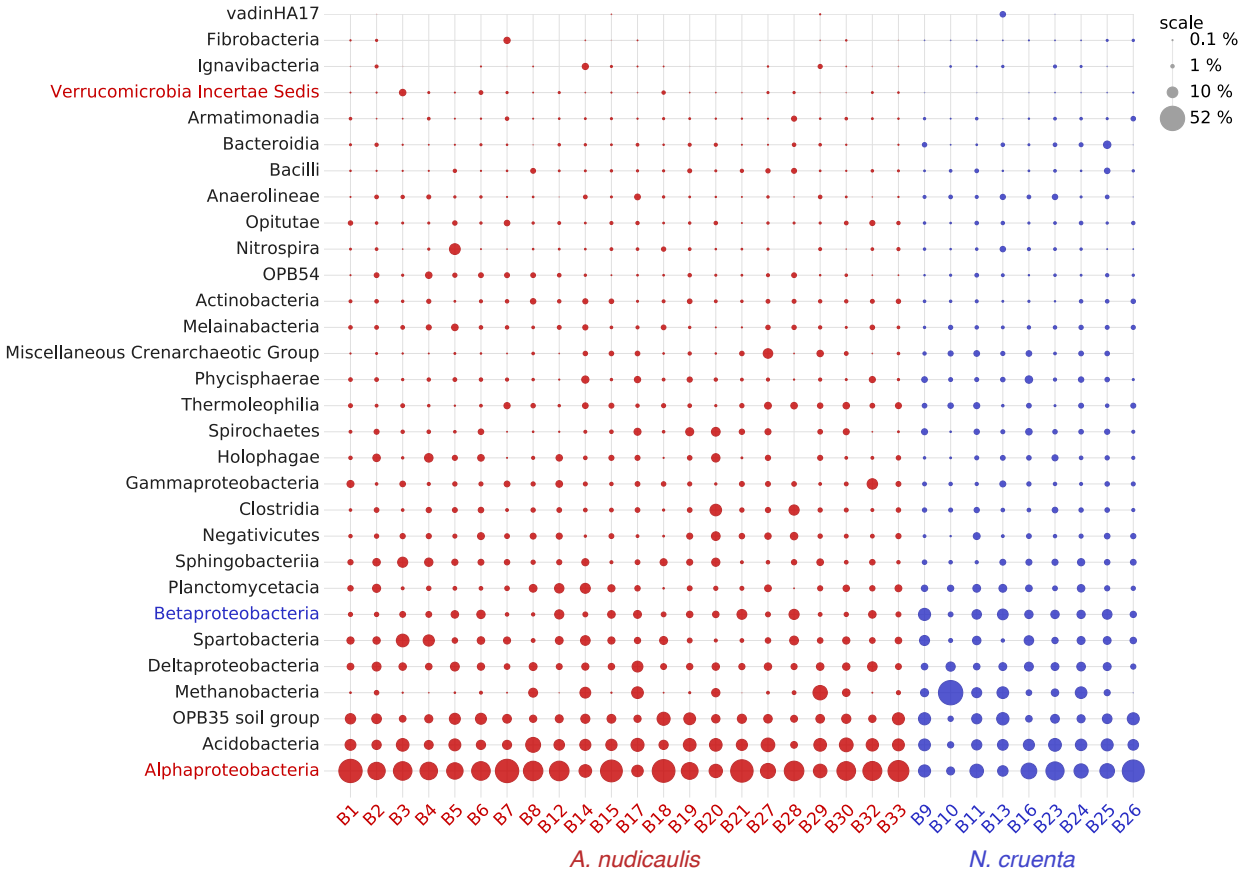

Figure S4: **Taxonomic community composition in bromeliads (class level).** Relative abundances of various prokaryotic classes (one columns per sample, one row per class). Circle surface is proportional to relative abundance. Only the class comprising at least 2% in at least one bromeliad are shown. Samples are colored according to bromeliad species (red for *A. nudicaulis* and blue for *N. cruenta*). Classes with statistically significant ($P < 0.05$ based on permutation tests) overrepresentation in *A. nudicaulis* or *N. cruenta* are indicated in red and blue, respectively. For profiles at the phylum, order and family level see Figs. S10, S11 and S3, respectively.

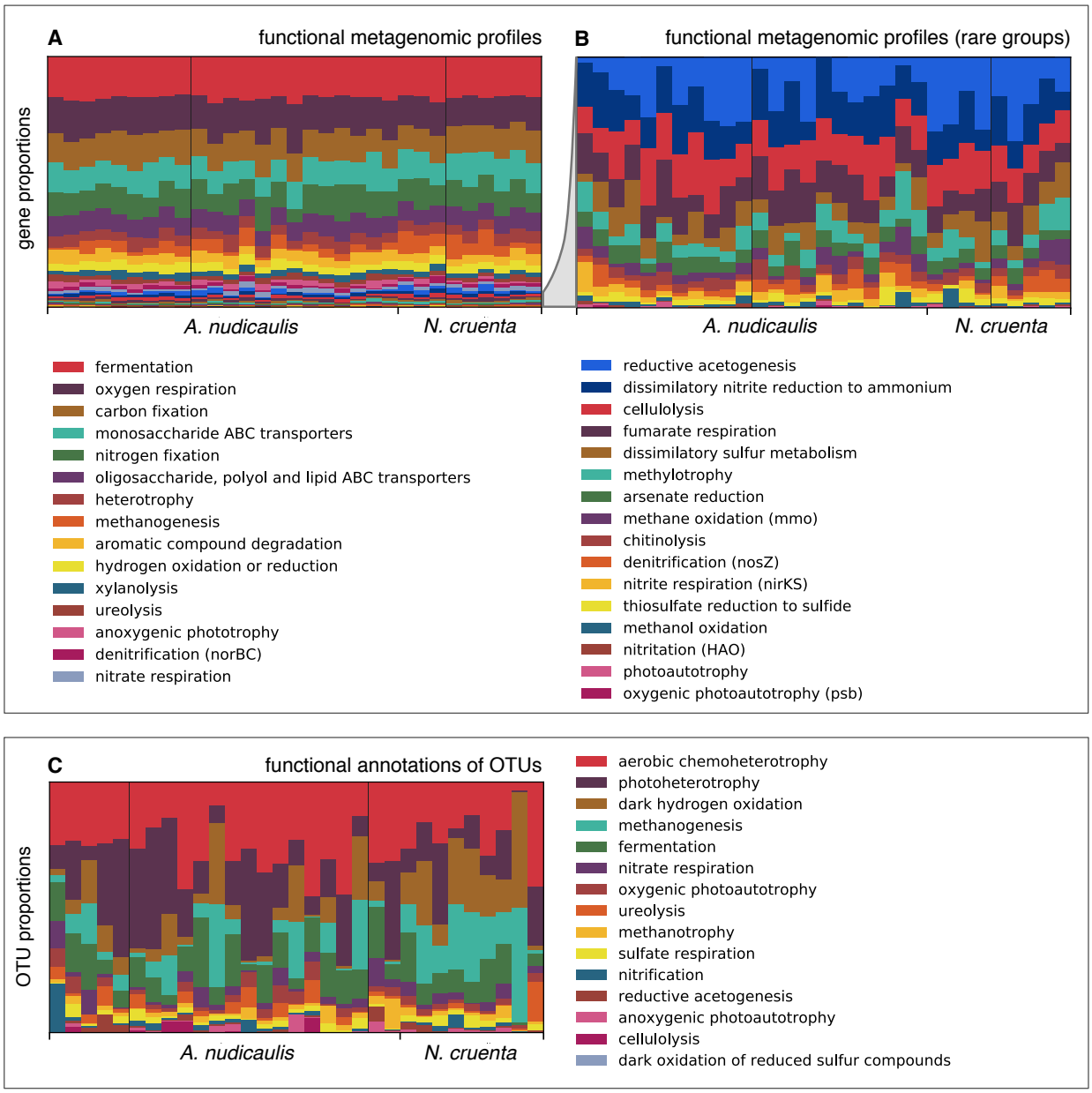

Figure S5: **Functional community profiles in bromeliads.** (A) Metagenomic functional profiles, in terms of relative gene abundances (one column per sample, one color per functional group). Most functional groups comprise several genes or several subunits of one gene. (B) Same as (A), but only showing the 15 least abundant functional groups. For the list of genes (KEGG orthologs) included in each group, see Supplemental Table S4. (C) Relative abundances of OTUs associated with various metabolic functions, used to facilitate the interpretation of metagenomic functional profiles.

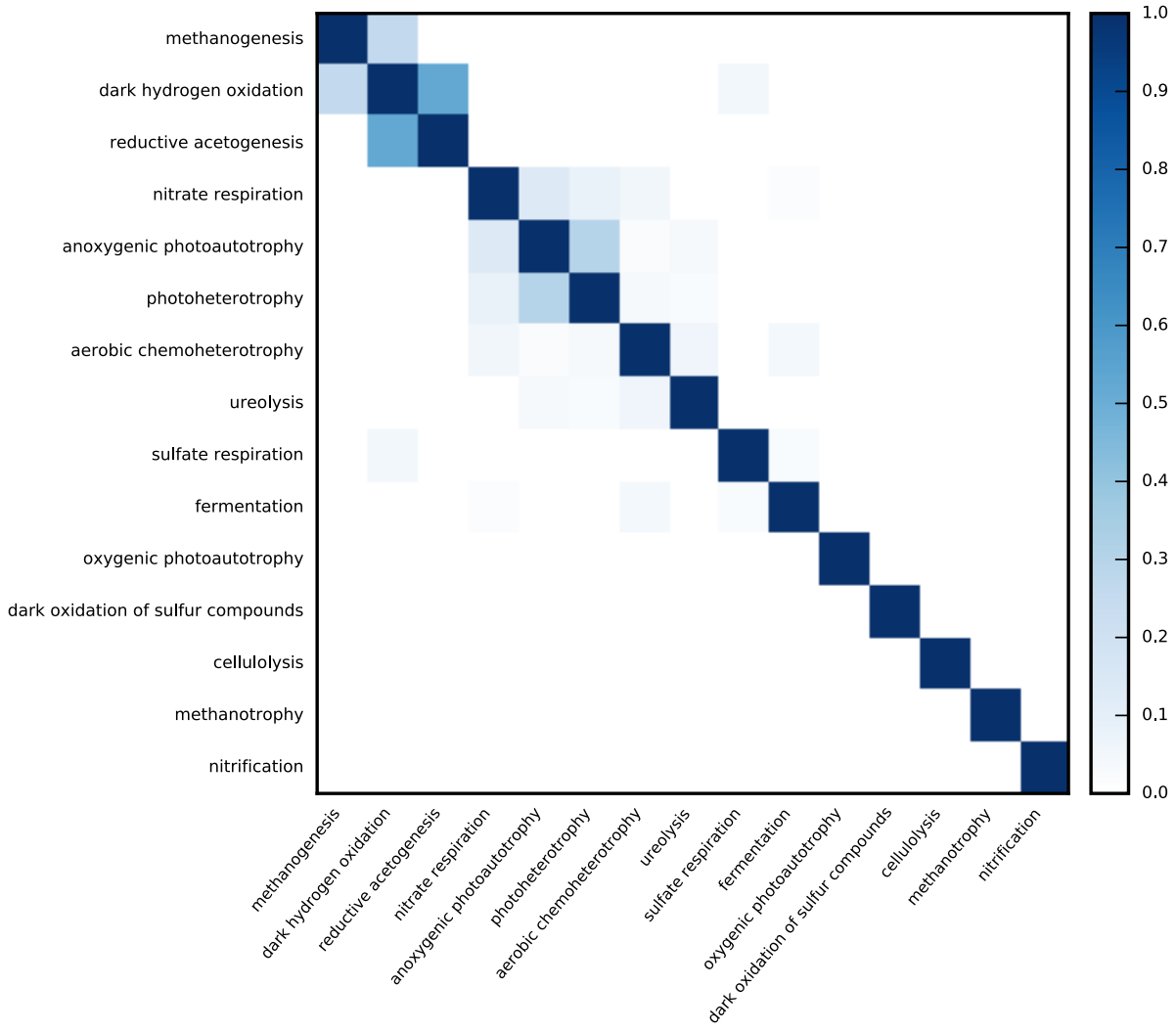

Figure S6: **Ambiguities in functional annotations of OTUs across bromeliads.** Overlaps between prokaryotic functional groups in terms of shared identified OTUs (Jaccard similarity index). A darker color corresponds to a greater overlap. An overlap of 1.0 corresponds to identical groups.

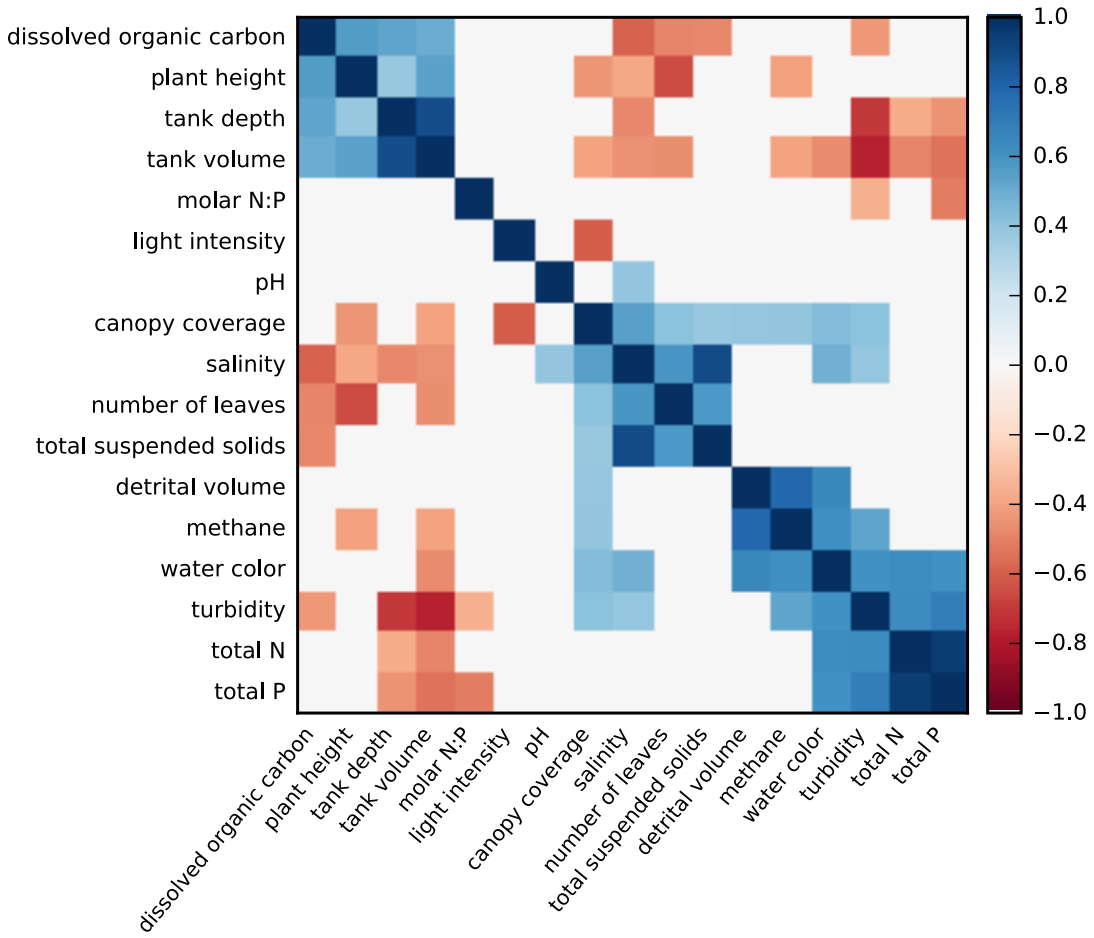

Figure S7: **Correlations between environmental variables across bromeliads.** Spearman rank correlations between environmental variables across all bromeliads. Blue and red correspond to statistically significant ($P < 0.05$) positive and negative correlations, respectively. White indicates zero or statistically non-significant correlations. Rows and columns are hierarchically clustered by similarity.

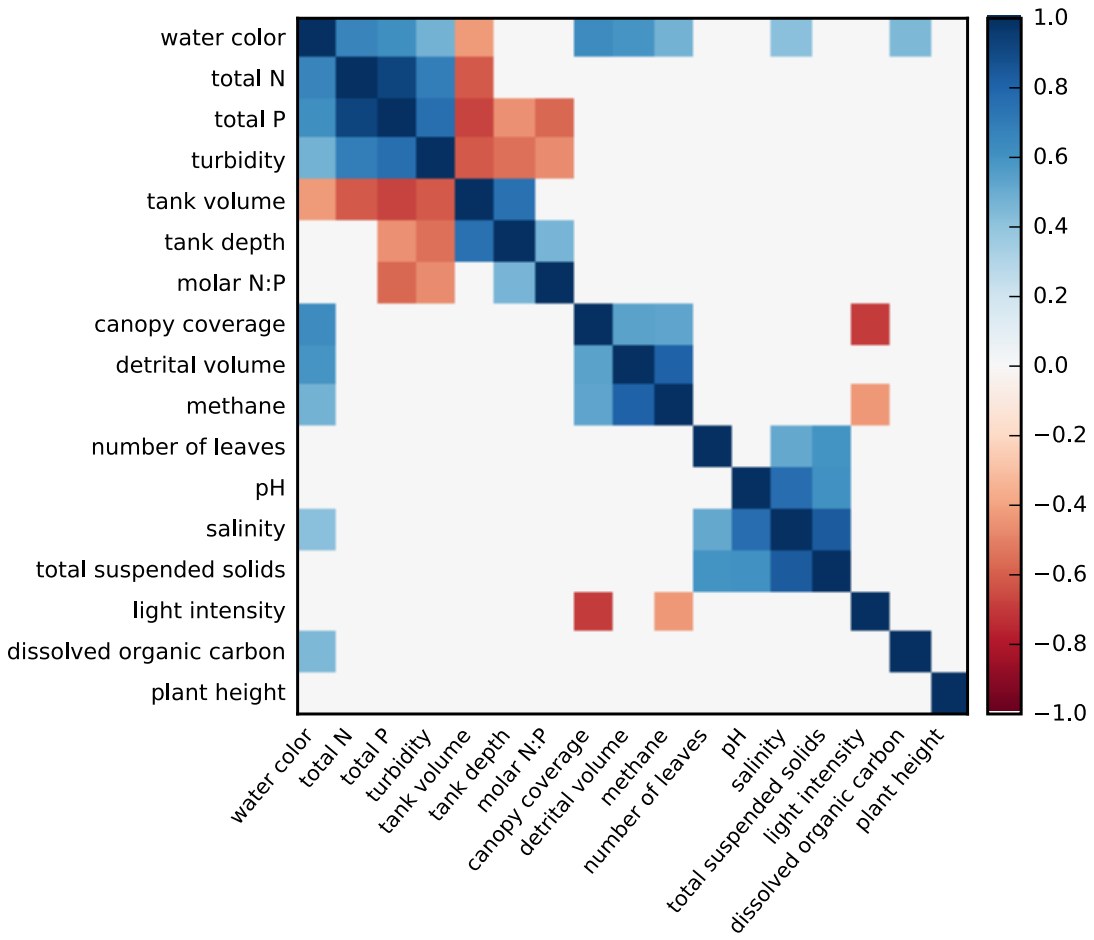

Figure S8: **Correlations between environmental variables (within *A. nudicaulis*).** Spearman rank correlations between environmental variables across *A. nudicaulis* bromeliads. Blue and red correspond to statistically significant ($P < 0.05$) positive and negative correlations, respectively. White indicates zero or statistically non-significant correlations. Rows and columns are hierarchically clustered by similarity. For correlations across all bromeliads (*A. nudicaulis* and *N. cruenta*), see Fig. S7.

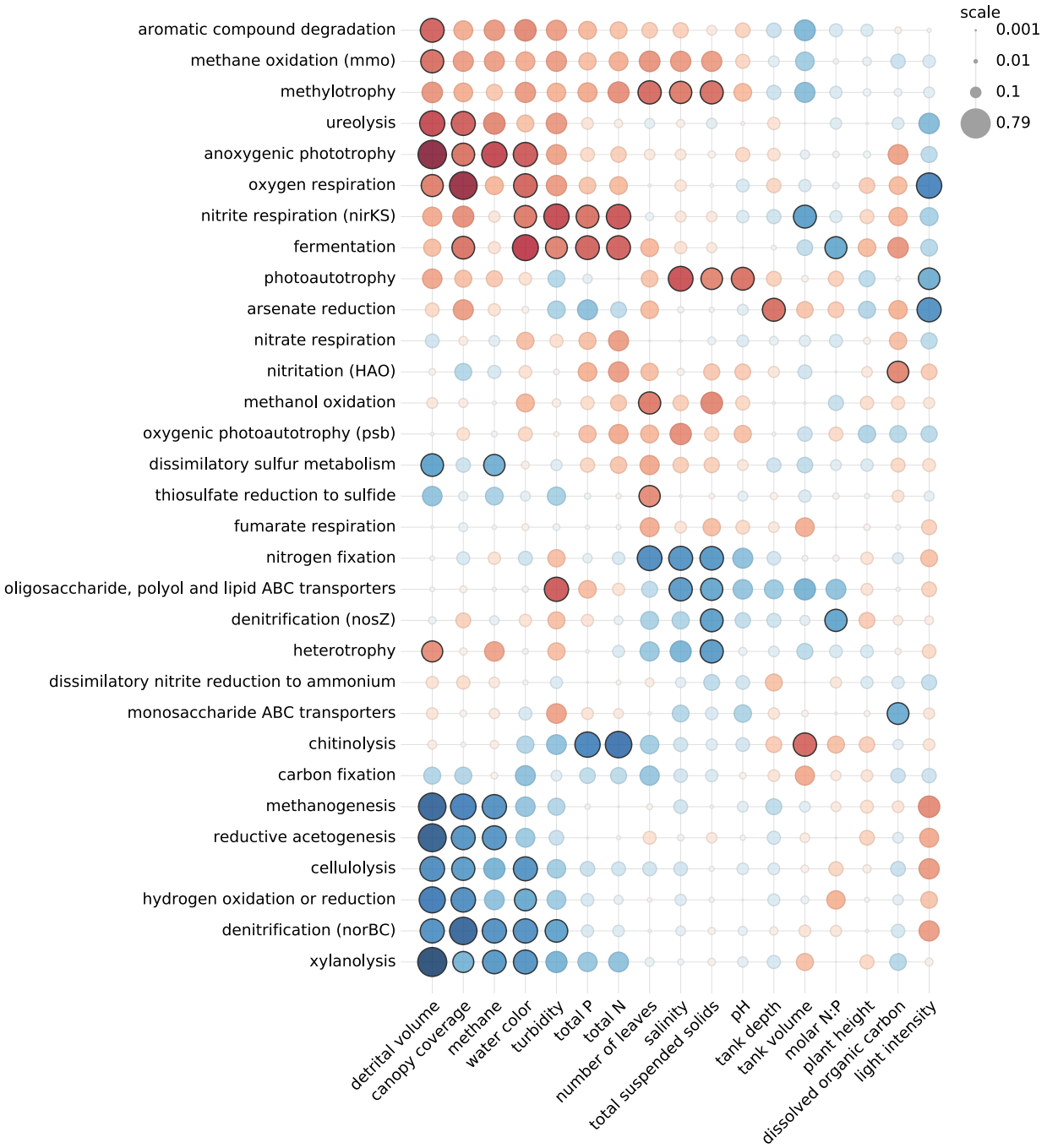

Figure S9: **Metagenomic functional groups vs environmental variables (within *A. nudicaulis*).** Spearman rank correlations between relative metagenomic functional group abundances and environmental variables across *A. nudicaulis* bromeliads. Blue and red colors correspond to positive and negative correlations, respectively. Circle size and color saturation are proportional to the magnitude of the correlation. Statistically significant correlations ($P < 0.05$) are indicated by black perimeters. Rows and columns are hierarchically clustered by similarity. For correlations across all bromeliads (*A. nudicaulis* and *N. cruenta*), see Fig. 3.

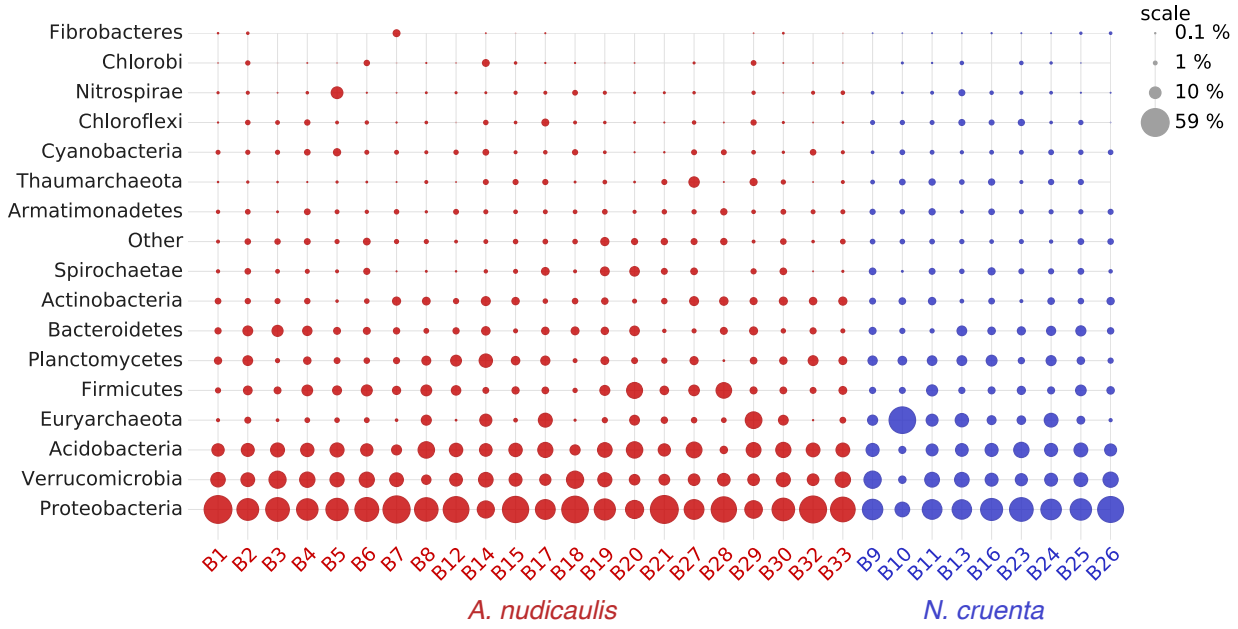

Figure S10: **Taxonomic community composition in bromeliads (phylum level).** Relative abundances of various prokaryotic phyla (one column per sample, one row per phylum). Circle sizes are proportional to relative abundances. Only the most abundant phyla (i.e. comprising at least 2% in at least one sample) are shown. None of the shown phyla exhibited a significant overrepresentation in any bromeliad species. For profiles at the class, order or family level, see Figs. S4, S11 and S3, respectively.

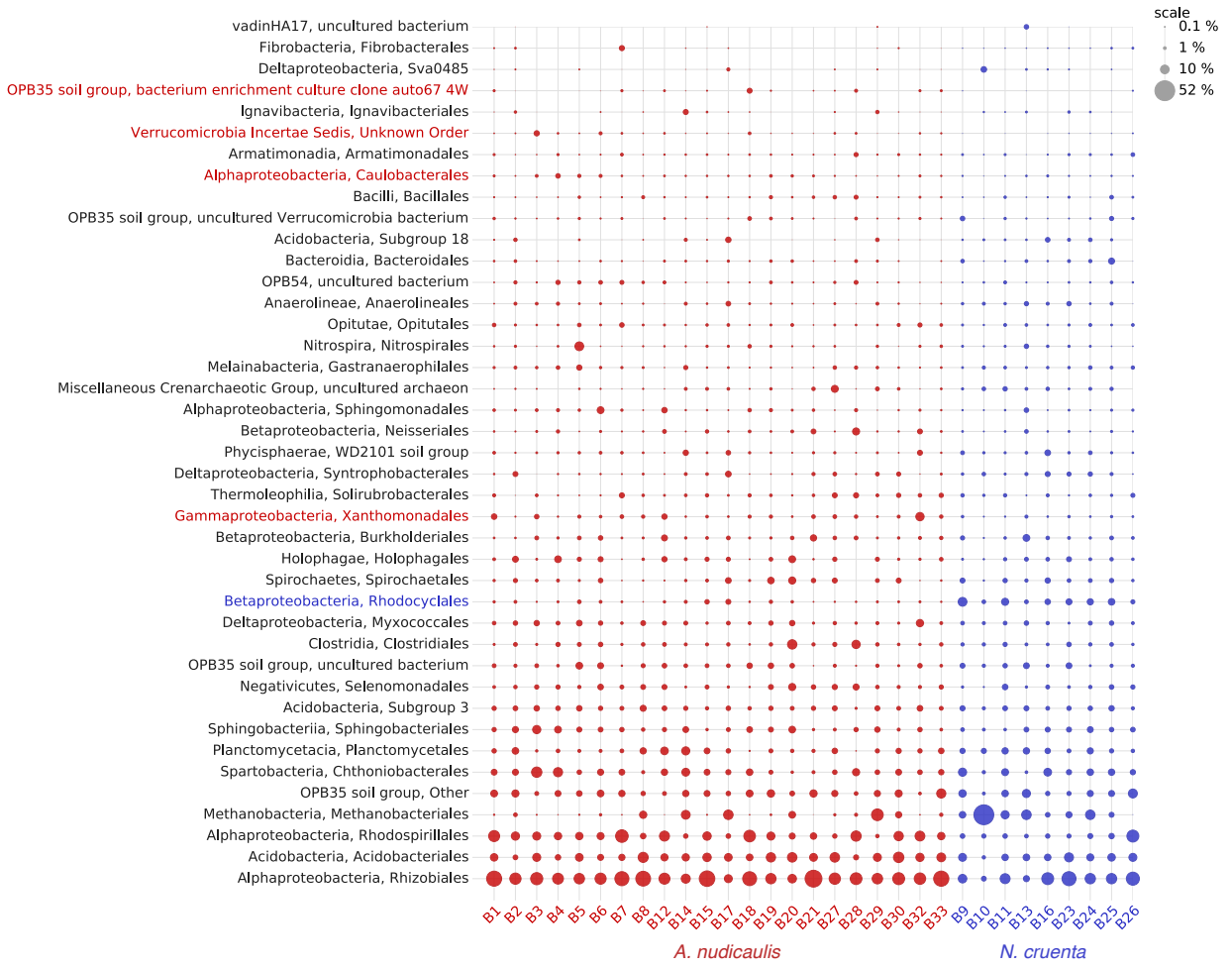

Figure S11: **Taxonomic community composition in bromeliads (order level).** Relative abundances of various prokaryotic orders (one column per sample, one row per order). Circle sizes are proportional to relative abundances. Only the most abundant orders (i.e. comprising at least 2% in at least one sample) are shown. Orders with statistically significant ($P < 0.05$) overrepresentation in *A. nudicaulis* or *N. cruenta* are indicated in red and blue, respectively. For profiles at the phylum, class or family level, see Figs. S10, S4 and S3, respectively.

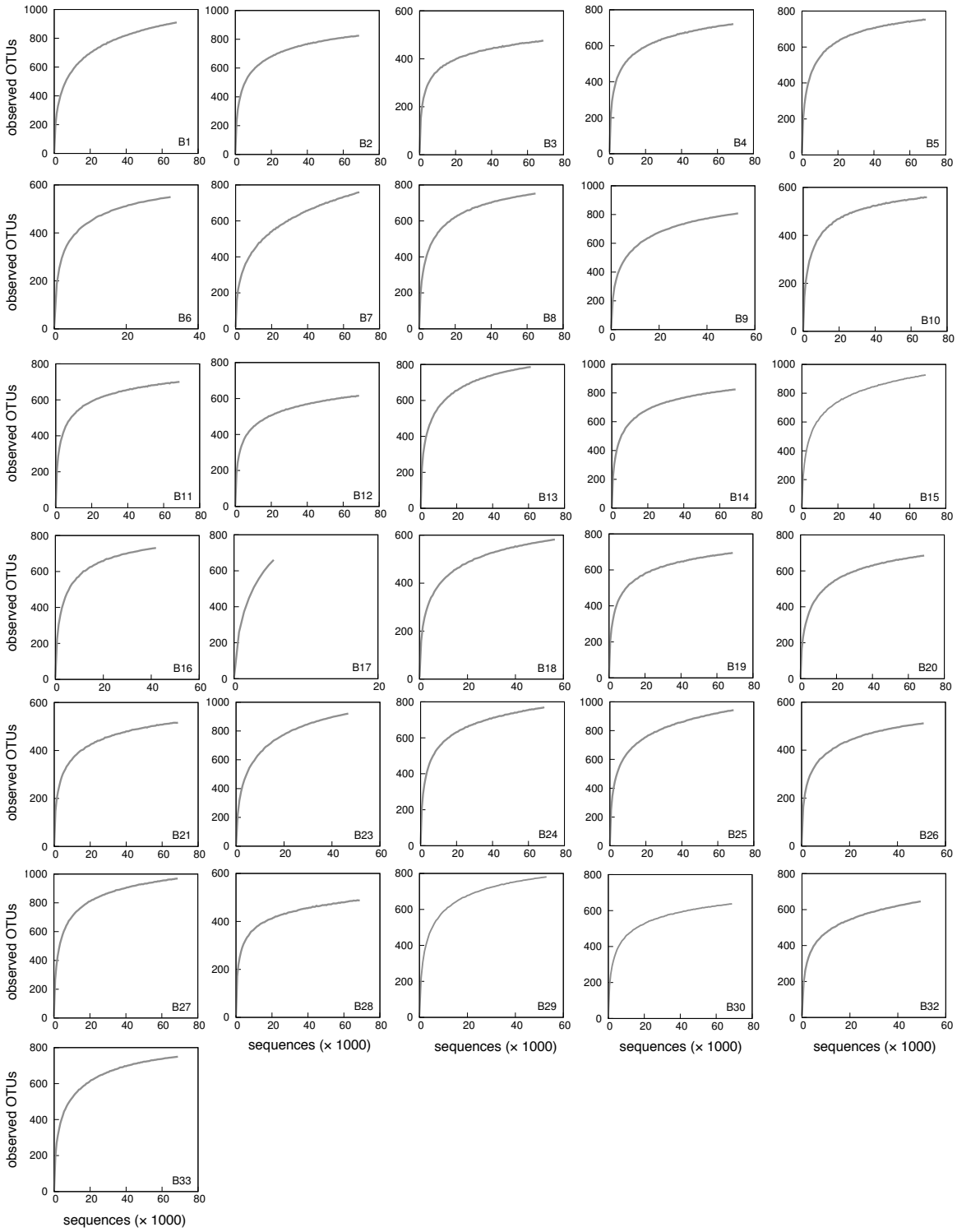

Figure S12: **16S rDNA rarefaction curves for bromeliads (OTU richness).** Each plot: Expected number of observed distinct OTUs at various sequencing depths for a particular bromeliad, determined through repeated random rarefactions. Bromeliad IDs are provided in the figures.

Table S1: **Comparisons between bromeliad species.** Statistical comparison of prokaryotic community structure between bromeliad species, *A. nudicaulis* and *N. cruenta*, in terms of the taxa, gene groups (as listed in Fig. 2A), KEGG orthologous groups (KOG) and KEGG categories (level B & C). Also listed are the fractions of taxa, gene groups, KOGs or KEGG categories whose mean relative abundances differed significantly ($P < 0.05$) between the two bromeliad species.

aspect	**statistics**	**pattern**
metag. functional groups	PERMANOVA of Bray-Curtis dissimilarities	separate, $P = 0.002$
KOG	PERMANOVA of Bray-Curtis dissimilarities	separate, $P = 0.009$
KEGG (level B)	PERMANOVA of Bray-Curtis dissimilarities	separate, $P = 0.006$
KEGG (level C)	PERMANOVA of Bray-Curtis dissimilarities	separate, $P = 0.01$
OTUs	PERMANOVA of Bray-Curtis dissimilarities	separate, $P < 0.001$
genera	PERMANOVA of Bray-Curtis dissimilarities	separate, $P = 0.003$
families	PERMANOVA of Bray-Curtis dissimilarities	separate, $P = 0.003$
orders	PERMANOVA of Bray-Curtis dissimilarities	separate, $P = 0.01$
classes	PERMANOVA of Bray-Curtis dissimilarities	separate, $P = 0.008$
phyla	PERMANOVA of Bray-Curtis dissimilarities	separate, $P = 0.031$
metag. functional groups	permutation tests for means of each group	13% signif. different
KOG	permutation tests for means of each KOG	15% signif. different
KEGG (level B)	permutation tests for means of each category	51% signif. different
KEGG (level C)	permutation tests for means of each category	23% signif. different
OTUs	permutation tests for means of each OTU	18% signif. different
genera	permutation tests for means of each genus	18% signif. different
families	permutation tests for means of each family	15% signif. different
orders	permutation tests for means of each order	11% signif. different
classes	permutation tests for means of each class	7.7% signif. different
phyla	permutation tests for means of each phylum	5.7% signif. different

Table S2: **Overview of 3rd party samples.** Overview of freshwater sediment and soil 16S sequencing samples obtained from the Earth Microbiome Project (EMP, `http://www.earthmicrobiome.org`), for comparison with the bromeliads. The table includes the original EMP sample IDs, as well as run accessions at the European Nucleotide Archive (`http://www.ebi.ac.uk/ena`) and the original publication (if available). Metadata were obtained from the accessions, the original publication or from the EMP database (`ftp.microbio.me/emp`).

EMP sample ID	location	lat. (°)	lon. (°)	depth (cm)	date (Y.M.D)	accession	publication
1039.L.Jacarepia.SB.1.6	Jacarepia Lake, Brazil	-23.14	-44.17	0	2011.01.24	ERR1557982	-
1622.DP.15.16B	Doe Pond, MA, USA	42.18	-72.7	16	-	ERR1538563	-
1622.DP.21.22B	Doe Pond, MA, USA	42.18	-72.7	22	-	ERR1538569	-
1622.UPMain.9.10	Uncas Pond, MA, USA	42.06	-71.38	10	-	ERR1538777	-
1622.UPMain.11.12B	Uncas Pond, MA, USA	42.06	-71.38	12	-	ERR1538636	-
1622.PP.11.12B	Pickerel Pond, MA, USA	42.31	-71.34	12	-	ERR1538589	-
1627.LC	Lang Co Lake, Tibetan Plateau	29.21	87.4	5	2010	ERR1589920	Xiong *et al.* (2012)
1627.RWC	Ranwu Co Lake, Tibetan Plateau	29.45	96.79	5	2010	ERR1589923	Xiong *et al.* (2012)
1627.SMXC	Sumxi Co Lake, Tibetan Plateau	34.6	80.25	5	2010	ERR1589924	Xiong *et al.* (2012)
632.Agricultural.soil.soy	agric. soil (soy), ON, Canada	43.63	-80.39	0–10	NA	ERR1742397	Neufeld *et al.* (2011)
632.Agricultural.soil.wheat	agric. soil (wheat), ON, Canada	43.64	-80.41	0–10	NA	ERR1742398	Neufeld *et al.* (2011)
1001.SKB1	agric. soil (Cannabis), CA, USA	33.19	-117.24	20	2011.11	ERR1543746	Winston *et al.* (2014)
1001.SKB2	agric. soil (Cannabis), CA, USA	33.19	-117.24	20	2010.11	ERR1543747	Winston *et al.* (2014)
1711.KAJ7.1	agric. soil, Western Kenya	0.15	35.52	20	2012.06	-	Wood *et al.* (2015)
1711.KAJ8.1	agric. soil, Western Kenya	0.15	35.52	20	2012.06	-	Wood *et al.* (2015)
1711.KAJ9.1	agric. soil, Western Kenya	0.15	35.52	20	2012.06	-	Wood *et al.* (2015)
808.AK.19.12a.s.4.1.sequences	taiga soil, AK, USA	65.15	-147.50	0–10	2009.06.29	ERR1759864	Kao *et al.* (2012)
808.AK.19.15a.s.4.1.sequences	taiga soil, AK, USA	65.15	-147.50	0–10	2009.06.29	ERR1759866	Kao *et al.* (2012)

Table S3: **Comparing taxon occurrences in bromeliads to lake sediments and soil.** Fractions of taxa whose occurrence frequency (i.e. the number of samples in which they were detected) differed significantly ($P < 0.05$) between bromeliads and freshwater lake sediments, or between bromeliads and soil. Statistical significances were calculated using the Welch statistic and permutation tests.

taxonomic level	**fraction of signif. diff. taxa in lake sediments**	**fraction of signif. diff. taxa in soil**
genus	34.1% (534 out of 1567)	39.4% (570 out of 1445)
family	38.5% (337 out of 875)	43.6% (305 out of 700)
order	39.1% (190 out of 486)	43.5% (143 out of 329)
class	40.6% (95 out of 234)	41.4% (60 out of 145)
phylum	31.9% (22 out of 69)	35.0% (14 out of 40)

Table S4: **KOG-function associations.** KEGG gene orthologous groups (KOG) associated with various functions in the metagenomic sequences.

function	KOG
anoxygenic phototrophy	K08944, K08940, K08941, K08942, K08943, K08946, K08945, K08947, K08948, K08949, K08950, K08951, K08952, K08953, K08954, K08926, K08927, K08928, K08929, K13991, K13992, K13994, K08939, K08930
aromatic compound degradation	K15760, K15761, K15762, K15763, K15764, K15765, K00055, K00141, K15757, K15758, K00055, K00141, K10616, K18293, K10617, K10618, K03268, K16268, K18089, K18090, K16269, K16249, K16243, K16244, K16242, K16245, K16246, K05549, K05550, K05784, K05783, K05599, K05600, K11311, K16319, K16320, K18248, K18249, K03381, K01856, K03464, K01055, K14727, K00446, K07104, K10217, K01821, K01617, K10216, K18364, K02554, K18365, K01666, K18366, K04073, K10619, K16303, K16304, K18227, K10620, K10621, K10622, K10623, K08689, K15750, K18087, K18088, K08690, K00462, K10222, K15751, K15752, K15753, K15754, K15755, K15756, K07540, K07543, K07544, K07545, K07546, K07547, K07548, K07549, K07550, K04112, K04113, K04114, K04115, K19515, K19516, K07537, K07538, K07539, K04116, K04117, K07534, K07535, K07536, K14579, K14580, K14578, K14581, K14582, K14583, K14584, K14585, K00152, K18242, K18243, K14578, K14581, K18074, K18075, K18077, K18076, K18068, K18069, K18067, K04102, K18251, K18252, K18253, K18254, K18255, K18256
arsenate reduction	K00537, K03741
carbon fixation	K01595, K01601, K01602, K03737
cellulolysis	K19356, K19357, K01179, K01225, K19668
chitinolysis	K01183, K13381, K01452, K17523
denitrification (norBC)	K04561, K02305
denitrification (nosZ)	K00376
dissimilatory nitrite reduction to ammonium	K00362, K00363, K03385, K15876
dissimilatory sulfur metabolism	K11180, K11181, K00394, K00395, K17219, K17220, K17221, K16952, K17222, K17223, K17224, K17225, K17226, K17227
fermentation	K01568, K13951, K00114, K00002, K04022, K00128, K00129, K00016, K00102, K00656, K00825, K00004, K00929, K00248, K00239, K00240, K00241, K00242
fumarate respiration	K00244, K00245

Table S4: Continued from previous page.

function	KOG
heterotrophy PTS	K08483, K02784, K02777, K02778, K02779, K02802, K02803, K02804, K02790, K02791, K02763, K02764, K02765, K02808, K02809, K02810, K02755, K02756, K02757, K02752, K02753, K02817, K02818, K02819, K11191, K11192, K02749, K02750, K02786, K02787, K02788, K02759, K02760, K02761, K02798, K02799, K02800, K11198, K11199, K11200, K02793, K02794, K02795, K02796, K19506, K19507, K19508, K19509, K11194, K11195, K11196, K02771, K02812, K02813, K02814, K02815, K02744, K02745, K02746, K02747, K10984, K10985, K10986, K17464, K17465, K17466, K17467, K02781, K02782, K02783, K02773, K02774, K02775, K02821, K02822, K03475, K11183, K02768, K02769, K02770, K08484, K08485, K02806
hydrogen oxidoreduction	K00532, K00533, K00534, K06441, K18016, K18017, K18023, K00436, K05586, K05587, K05588, K18005, K18006, K18007
methane oxidation (mmo)	K16157, K16158, K16159, K16160, K16161, K16162, K08684
methanogenesis	K00399, K00401, K00402, K03421, K03422, K03388, K03389, K03390
methanol oxidation	K14028, K14029, K17066, K16254, K16255, K16256, K16257, K16258, K16259, K16260, K00093, K17066
methylotrophy	K14028, K14029, K17066, K16254, K16255, K16256, K16257, K16258, K16259, K16260, K00093, K17066, K16157, K16158, K16159, K16160, K16161, K16162, K10713, K14028, K14029, K17066
monosaccharide ABC transporters	K10196, K10197, K10198, K10199, K17315, K17316, K17317, K10439, K10440, K10441, K06726, K10537, K10538, K10539, K10540, K10541, K10542, K10543, K10544, K10545, K10549, K10550, K10551, K10552, K10553, K10554, K10555, K10556, K10557, K10558, K10559, K10560, K10561, K10562, K17202, K17203, K17204, K17205, K17206, K17207, K17208, K17209, K17210, K17237, K17238, K17239, K17240, K17321, K17322, K17323, K17325, K17324, K05813, K05814, K05815, K05816, K10112
nitrate respiration	K02567, K02568, K00370, K00371, K00374, K00373
nitritation (HAO)	K10535
nitrite respiration (nirKS)	K00368, K15864
nitrogen fixation	K02588, K02586, K02591, K00531

Table S4: Continued from previous page.

function	KOG
oligosaccharide polyol and lipid ABC transporters	K10108, K10109, K10110, K10111, K15770, K15771, K15772, K10117, K10118, K10119, K10112, K10188, K10189, K10190, K10191, K10227, K10228, K10229, K10111, K10232, K10233, K10234, K10235, K10192, K10193, K10194, K10195, K17241, K17242, K17243, K17318, K17319, K17320, K10236, K10237, K10238, K17311, K17312, K17313, K17314, K10200, K10201, K10202, K10240, K10241, K10242, K10112, K17329, K17330, K17331, K17244, K17245, K17246, K17234, K17235, K17236, K17326, K17327, K17328, K10546, K10547, K10548, K07323, K02067, K02066, K07122, K02065
oxygen respiration (cox)	K02277, K02276, K02274, K15408, K02275, K02262, K02256, K02261, K02263, K02264, K02265, K02266, K02267, K02268, K02269, K02270, K02271, K02272, K02273, K02258, K02259, K02260, K00404, K00405, K15862, K00407, K00406, K02259, K02259, K00406, K00407, K00405, K00404, K00425, K00426
oxygenic photosynthesis (photosystem II)	K02703, K02704, K02705, K02706, K02707, K02708, K02709, K02710, K02711, K02712, K02713, K02714, K02716, K02717, K02718, K02719, K02720, K02721, K02722, K02723, K02724, K03541, K03542, K08901, K08902, K08903, K08904
photosynthesis	K02703, K02704, K02705, K02706, K02707, K02708, K02709, K02710, K02711, K02712, K02713, K02714, K02716, K02717, K02718, K02719, K02720, K02721, K02722, K02723, K02724, K03541, K03542, K08901, K08902, K08903, K08904, K02638, K02639, K02641, K02689, K02690, K02691, K02692, K02693, K02694, K02695, K02696, K02697, K02698, K02699, K02700, K02701, K02702, K08905, K08906, K14332
reductive acetogenesis	K00192, K00195, K00193, K00194, K00197
thiosulfate reduction to sulfide	K08352, K08353, K08354
ureolysis	K01427, K01428, K01429, K01430, K14048, K14541, K01457, K01941
xylanolysis	K15924, K13465, K01198, K15920, K01181

Table S5: **Numbers of functionally annotated OTUs in bromeliads.** Number of OTUs associated with each metabolic function, compared to the total number of taxonomically annotated OTUs. Some OTUs were associated with multiple functions (Fig. S2).

functional group	OTUs	fraction (%)
aerobic chemoheterotrophy	237	11.6
anoxygenic photoautotrophy	7	0.34
cellulolysis	14	0.68
dark hydrogen oxidation	21	1.03
dark oxidation of sulfur compounds	3	0.15
fermentation	109	5.32
methanogenesis	13	0.64
methanotrophy	16	0.78
nitrate respiration	19	0.93
nitrification	13	0.64
oxygenic photoautotrophy	55	2.69
photoheterotrophy	19	0.93
reductive acetogenesis	11	0.54
sulfate respiration	44	2.15
ureolysis	23	1.12

References

Kao, R.H., Gibson, C.M., Gallery, R.E., Meier, C.L., Barnett, D.T., Docherty, K.M., *et al.* (2012) Neon terrestrial field observations: designing continental-scale, standardized sampling. *Ecosphere* **3**: 1–17.

Neufeld, J.D., Engel, K., Cheng, J., Moreno-Hagelsieb, G., Rose, D.R., and Charles, T.C. (2011) Open resource metagenomics: a model for sharing metagenomic libraries. *Standards in Genomic Sciences* **5**: 203–210.

Winston, M.E., Hampton-Marcell, J., Zarraonaindia, I., Owens, S.M., Moreau, C.S., Gilbert, J.A., *et al.* (2014) Understanding cultivar-specificity and soil determinants of the cannabis microbiome. *PloS One* **9**: e99641.

Wood, S.A., Bradford, M.A., Gilbert, J.A., McGuire, K.L., Palm, C.A., Tully, K.L., *et al.* (2015) Agricultural intensification and the functional capacity of soil microbes on smallholder african farms. *Journal of Applied Ecology* **52**: 744–752.

Xiong, J., Liu, Y., Lin, X., Zhang, H., Zeng, J., Hou, J., *et al.* (2012) Geographic distance and ph drive bacterial distribution in alkaline lake sediments across tibetan plateau. *Environmental microbiology* **14**: 2457–2466.